NASA Technical Paper 1136

Effect of Cooling-Hole Geometry on Aerodynamic Performance of a Film-Cooled Turbine Vane Tested With Cold Air in a Two-Dimensional Cascade

John F. Kline, Roy G. Stabe, and Thomas P. Moffitt

MARCH 1978

NASA

NASA Technical Paper 1136

Effect of Cooling-Hole Geometry on Aerodynamic Performance of a Film-Cooled Turbine Vane Tested With Cold Air in a Two-Dimensional Cascade

John F. Kline, Roy G. Stabe,
and Thomas P. Moffitt
Lewis Research Center
Cleveland, Ohio

NASA
National Aeronautics
and Space Administration

Scientific and Technical
Information Office

1978

EFFECT OF COOLING-HOLE GEOMETRY ON AERODYNAMIC PERFORMANCE OF A FILM-COOLED TURBINE VANE TESTED WITH COLD AIR IN A TWO-DIMENSIONAL CASCADE

by John F. Kline, Roy G. Stabe, and Thomas P. Moffitt

Lewis Research Center

SUMMARY

The effect of film-cooling hole size and orientation on aerodynamic losses attributable to film cooling the entire surface of a turbine vane was investigated in a two-dimensional cascade. In addition, the contribution of individual regions of the surface to the overall effects was determined.

A representative cooling-hole configuration consisting of 45 rows of holes equally spaced about the vane profile was used as a starting point. Nominal hole diameters of 0.0254 and 0.0356 centimeter and nominal hole orientations of 35°, 45°, and 55° from the local vane surface and 0°, 45°, and 90° from the main-stream flow direction were investigated. Ambient-temperature air was used for both cascade and coolant. The principal measurements were surveys of vane-exit flow conditions. Tests were made over a range of coolant to cascade-inlet total pressure ratio at design exit ideal critical velocity ratio, and over a range of exit ideal critical velocity ratio at a total-pressure ratio of 1.0.

An evaluation and comparison of cooling-hole geometry effects was made for flow conditions at design aftermix ideal critical velocity ratio and a coolant total to primary-air inlet total pressure ratio of 1.0. Aerodynamic performance was expressed in terms of the percent decrease in thermodynamic efficiency of the test vane below the value for an uncooled (solid) vane, per percent coolant ejected. This measure of performance is called the loss ratio. For coolant ejection from the pressure surface region or from the accelerating (forward) region of the suction surface, the loss ratio is relatively insensitive to the angle relative to the direction of main-stream flow. For coolant ejection from the diffusing (rear) region of the suction surface, the loss ratio is high and very sensitive to ejection angle from streamwise. For coolant ejection from the entire vane surface, the loss ratio is lowest for ejection in line with the main-stream flow from large holes at the minimum angle with the local surface. The loss ratio is fairly sensitive to spanwise ejection angle, and is somewhat lower for larger diameter holes. Coolant flow rates for ejection from individual regions can be added to obtain a very close prediction of flow rates for ejection from the entire surface. This was also true, in general, for losses.

Reference material indicates that compound-angle ejection provides better film coverage than does ejection in line with the main-stream flow. It appears that use of compound-angle ejection in the pressure region and accelerating region would have comparatively little effect on loss ratio. In the diffusing region, however, ejection at a compound angle would involve a compromise between cooling performance and aerodynamic loss.

Minimum values of loss ratio occurred at ejection total-pressure ratios above 1.0 for all configurations and all regions. These minimums were quite pronounced for 45° compound-angle and spanwise ejection, making the loss comparison with streamwise ejection more favorable in the pressure-ratio range available to second-stage blading.

INTRODUCTION

An extensive research program is in progress at the Lewis Research Center to investigate the effect of coolant ejection from the surfaces of turbine blades upon the aerodynamic performance of the turbine. As part of this program, cooled turbine vane performance is being measured experimentally in a two-dimensional cascade with cold air at a coolant- to cascade-inlet temperature ratio of 1.0. Coolant-ejection schemes involving trailing-edge ejection and blade-surface transpiration have been evaluated (ref. 1). Work is now in progress on film cooling from discrete holes. The effects of single-row and multiple-row hole configurations and various hole sizes are reported in references 2 to 4. These investigations were for coolant holes slanted 35° from the vane surface in the direction of the main-stream flow. Recent flow-visualization studies on flat plates (ref. 5) have shown that coolant ejection at an angle with both the vane surface and the main stream (compound-angle ejection) provides better film coverage.

The determination of the effect of this compound-angle ejection on turbine-vane aerodynamic performance is one of the principal objects of this investigation. Also included are the effects of ejection angle from the local vane surface and coolant hole size. The contribution of individual vane regions to the overall effect was also investigated. A representative full-coverage film hole location configuration for the entire surface of a turbine vane, consisting of 45 rows of 0.0254-centimeter-diameter holes equally spaced about the vane profile, a nominal hole diameter of 0.0254 centimeter, and a nominal hole spacing of 10 diameters, was used for this study. Nominal coolant-hole orientations of 35°, 45°, and 55° from the local vane surface in the direction of the main-stream flow and orientations of 15° and 35° from the local vane surface at angles of 45° and 90° from the main-stream flow direction were tested. The effect of hole size was investigated by halving the number of holes per row and doubling the area of each hole, so that the same coolant flow rate was obtained. Tests were made with ejection from holes in a number of vane surface regions, with holes in all other regions plugged and leveled to give a smooth surface for each test configuration. The configurations were tested as the center vane in a cascade of seven full-scale vanes, with solid, uncooled vanes in the other six positions. Test conditions covered a range of aftermix ideal critical velocity ratios from 0.6 to 0.94 at a coolant to primary air inlet total pressure ratio of 1.0, and a range of coolant to primary air inlet total pressure ratio from 1.0 to 1.5 at an aftermix ideal critical velocity ratio of 0.81.

The principal measurements were cross-channel surveys of total pressure, static pressure, and flow angle downstream from the vane exit. The results include representative surveys and overall performance in terms of coolant fraction and thermodynamic efficiency.

SYMBOLS

p	absolute pressure, N/cm^2
T	absolute temperature, K
V	velocity, m/sec
w	flow rate per unit of vane span, (g/sec)/cm
Y	coolant fraction (w_c/w_p)
α	flow angle from axial direction, deg
δ	ratio of total pressure at cascade inlet (p_1') to U.S. standard sea-level atmospheric pressure (10.132 N/cm^2)
η	thermodynamic efficiency $\left\{w_t V_3^2 \middle/ \left[w_p(V_{id,3})_p^2 + w_c(V_{id,3})_c^2\right]\right\}$
$\sqrt{\theta_{cr}}$	ratio of cascade-inlet critical velocity $(V_{cr,1})$ to critical velocity of U.S. standard sea-level air (310.6 m/sec)
φ	angle between cooling-hole axis and local vane surface (see fig. 2), deg
ψ	angle between cooling-hole axis and main-stream flow direction (see fig. 2), deg

Subscripts:

A	accelerating region of suction surface
c	coolant
cr	flow conditions at Mach 1 (critical)
D	diffusing region of suction surface
id	ideal, or isentropic, process
P	pressure-surface region
p	primary
T	trailing-edge region
t	total
0	noncooled (solid) vane
1	station at cascade inlet
2	station at vane-exit survey plane

3 station downstream of survey station, where flow conditions are assumed to be uniform ("aftermix" station)

Superscript:

total-state condition

APPARATUS AND PROCEDURE

Vanes and Cascade

The first-stage stator mean-section configuration of the full-size turbine described in reference 6 was used in this investigation. The vane profile coordinates, the cascade geometry, and the design inlet and exit flow velocities and angles are shown in figure 1. The axial solidity of the cascade is 0.932 (axial chord, 3.823 cm; pitch, 4.100 cm). The test vanes are straight (non-twisted), 13.7 centimeters long, and hollow, with a 0.102-centimeter-thick wall.

Cooling-Hole Configurations

The eight cooling-hole configurations tested in this investigation are specified in table I and figure 2. Test configuration (i) was adapted from a representative, fully film-cooled turbine vane described in reference 7. The principal objectives of the adaptation were the duplication of coolant-ejection characteristics insofar as external vane aerodynamics are concerned, and the nominalization of the hole-configuration parameters over as much of the vane surface as possible. The resulting test configuration (i), shown in figure 3, has holes arranged in 45 rows around the vane profile. The holes are spaced about 0.254 centimeter apart in each row with the exception of rows 1, 2, 25, and 45, where the spacing is 0.127 centimeter. In each row, the holes are located spanwise between the holes of adjacent rows. For economy reasons, the hole pattern is limited to the center 7.62 centimeters of the 10.16 centimeters of vane inside the cascade tunnel. The holes are 0.0254 centimeter in diameter except in rows 1, 2, and 45, where the diameter is 0.0343 centimeter. The hole orientation relative to the local vane surface (angle φ in fig. 2) is 35° everywhere except in rows 2, 3, and 4, where physical limitations necessitated larger angles, and in rows 1 and 25, where the 90° angle of the reference configuration is obviously proper. All holes are oriented in the direction of the main-stream flow, so that the angle ψ (see fig. 2) is zero. The "nominal" geometry parameter values for test configuration (i) are as follows: hole diameter, 0.0254 centimeter; hole spacing, 0.254 centimeter; angle from surface, φ,

35^o; angle from streamwise, ψ, 0^o.

To study the effect of hole orientation relative to the local vane surface, the 35^o nominal angle from the vane surface, φ, of configuration (i) was increased to 45^o for configuration (ii), and to 55^o for configuration (iii). To determine the effect of hole size, the hole area of configuration (i) was doubled for configuration (iv), and the hole spacing was also doubled, to give the same coolant flow per row. To investigate the effect of hole orientation relative to the main-stream flow direction, the 0^o angle ψ of configuration (iv) was changed to 45^o for configuration (v), and to 90^o for configuration (vii). In addition, the 90^o angle from the vane surface (angle φ) of the row-1 holes of configuration (iv) was changed to the nominal value of 35^o for configurations (v) and (vii). The effect of a lower angle from the vane surface at a 45^o angle from the main-stream flow direction was investigated by reducing the 35^o nominal angle φ of configuration (v) to 20^o for configuration (vi). The effect of a lower angle from the vane surface at a 90^o angle from the main-stream direction was investigated by reducing the 35^o angle φ of configuration (vii) to 15^o for configuration (viii).

As shown in figure 2, the vane profile is divided into four basic regions: the pressure-surface region, P; the suction-surface accelerating region, A; the suction-surface diffusing region, D; and the trailing-edge region, T. To determine the loss ratio for coolant ejection from one particular vane surface region only, the holes in all the other regions were filled and the surface was leveled. To investigate the effect of ejection from multiple regions of the vane surface, combined regions AD, PAT, and DT of configurations (iv), (v), (vi), and (viii) were tested.

To determine the reference efficiency for an uncooled vane (η_0), a solid vane having the same profile as the test vane was used.

Cascade Tunnel

All configurations were tested as the center vane in a seven-vane cascade in the 10.16-centimeter-span, ambient inlet, two-dimensional cascade tunnel shown in figure 4 and described in reference 8. The other six vanes were uncooled, solid airfoils with the test-vane profile. The validity of results for a single cooled vane in a cascade of uncooled vanes was investigated in reference 9 and approved for loss comparison of essentially similar cooling designs.

In operation, room air was drawn into the cascade-tunnel inlet and through the cascade of vanes by evacuating the chamber surrounding the cascade exit. The boundary layer was removed from the tunnel sidewall through flush slots just upstream of the vane leading edge. Metered cooling air at the temperature of tunnel-inlet air was supplied to both ends of the test vane and ejected from cooling holes in the vane surface.

Instrumentation

Flow conditions 1.27 centimeters axially downstream of the vane trailing edge were surveyed with the three-element combination probe shown in figure 5. This probe senses total pressure with a square-ended, 0.051-centimeter-diameter tube, static pressure with a 15^{o}-angle wedge, and flow angle with two tubes with ends cut at 45^{o}. The probe was calibrated frequently over the range of flow angles and velocities encountered in the test. The positioning of the probe relative to the cascade is indicated in figure 1. All surveys were made at the middle of the vane span. In operation, the probe was traversed parallel to the plane of the vane trailing edges at a speed of about 2.54 centimeters per minute. The pressures sensed by the three elements were measured and recorded, along with traverse position, five times per second (every 0.008 cm of survey).

The total pressure inside the test vane was sensed with a square-ended tube extending halfway through the inside of the vane. Cooling air flow was measured with an ASME flat-plate orifice. The temperatures of the air entering the cascade tunnel, the coolant entering the test vane, and the coolant at the orifice were measured with thermocouples. Tunnel inlet pressure, coolant total pressure inside the test vane, orifice pressures, and all temperatures were sampled once every 2 seconds. Average values for the duration of the survey were used in all computations.

Procedure

Preliminary measurements were made to determine if the survey results were sensitive to the spanwise position of the probe elements relative to the holes in the vane. The elements are spaced 0.508 centimeter apart to put each one in a similar position relative to the cooling-hole pattern on the vane. At design aftermix primary-air ideal critical velocity ratio and a coolant to primary-air inlet total-pressure ratio of 1.0, the spanwise variation in efficiency for the small-hole configuration (i) was about ±0.15 percentage point (±5.4 percent variation in efficiency loss ratio $(\eta_0 - \eta)/\eta_0 Y$). The variation in efficiency for the large-hole configuration (iv) was about ±0.45 percentage point (±18.4 percent variation in efficiency loss ratio). A spanwise position directly downstream from the holes of row 23 was found to give representative and stable results and was used for all tests. It was appreciated that ejection at an angle from streamwise would displace and alter this pattern and that the effect would be different for different coolant flow rates. However, establishment of the actual pattern for each coolant flow rate for each ejection configuration was considered impractical. In addition, it was felt that the efficiency variation would be less, due to the lower axial component of coolant velocity. This could still have produced some of the scatter encountered in the data for ejection at an angle from streamwise.

Each configuration was tested at aftermix primary-air ideal critical velocity ratios from 0.6 to 0.94 at a coolant to primary-air inlet total-pressure ratio p'_c/p'_1 of 1.0. In addition, tests were made at the design aftermix primary-air ideal critical velocity ratio of 0.81 over a range of coolant to primary-air inlet total-pressure ratio from the minimum value that would ensure outflow from all holes to a maximum value of 1.5. Exit survey readings were used to compute local flow conditions and quantities. These quantities were integrated numerically over a distance of one vane pitch to obtain total values. The continuity and conservation of energy and momentum relations were then used (ref. 10) to calculate the flow conditions at hypothetical aftermix station 3, where they are uniform.

RESULTS AND DISCUSSION

The relative effect of cooling-hole geometry parameters on the aerodynamic performance of a film-cooled turbine vane is reported. The effect, measured experimentally with cold air in a two-dimensional cascade, is expressed in terms of the percent loss in thermodynamic efficiency (from the value of 0.979 for the uncooled vane) for each percent of cooling air ejected from the vane surface. This quantity is termed efficiency loss ratio and is expressed in symbols as $(\eta_0 - \eta)/\eta_0 Y$. Complete test data for all configurations tested are presented in table II. Performance characteristics typical of all configurations are presented and discussed. The effects of hole size, hole angle from the vane surface, and hole angle from the main-stream flow direction upon efficiency loss ratio for a fully cooled vane are examined, and the contributions of individual vane regions to these effects are analyzed.

General Characteristics

Typical total-pressure, static-pressure, and flow-angle variations through the wake of an uncooled (solid) vane and a cooled vane (configuration (iv)) at the survey station are shown in figure 6. The data are for a nominal aftermix ideal critical velocity ratio $\left(V/V_{cr}\right)_{id,3}$ of 0.81 (design) and a nominal coolant to primary-air inlet total-pressure ratio p'_c/p'_1 of 1.0. The pressures have been normalized to primary-air total pressure p'_1 at the cascade inlet.

The total pressure of the cooled vane is lower in the wake than that of the uncooled vane (upper curves, fig. 6(a)); this indicates higher losses and, therefore, lower efficiency for the cooled vane. The total-pressure wake shown for the uncooled vane represents an efficiency of 0.979 for this test condition, and the larger total-pressure wake for the cooled vane represents an efficiency of 0.956. The width of the wake (as defined by reduced total pressure) is about the same for these configurations and was also about the same for all configurations.

The static-pressure variation (lower curves, fig. 6(a)) of the cooled vane is almost identical in shape to that of the uncooled vane. This was true for all cooled configurations. The slight difference in level of the static-pressure trace in this example is a result of typical variation of the test condition $\left(V/V_{cr}\right)_{id,3}$ from the nominal value.

The flow angle of the cooled vane (fig. 6(b)) varies more than that of the uncooled vane in the wake area. This variation is, however, still well within the $\pm 15^{\circ}$ calibration range of the survey probe.

Typical variation of equivalent total flow rate $w_t \sqrt{\theta_{cr}}/\delta$ and thermodynamic efficiency η with aftermix ideal critical velocity ratio $\left(V/V_{cr}\right)_{id,3}$ at a nominal coolant to primary-air inlet total-pressure ratio p'_c/p'_1 of 1.0 is shown in figure 7. Equivalent flow is based on primary-air conditions at the cascade inlet. Total flow of the two configurations (fig. 7(a)) is the same within 1.0 percent up to a velocity ratio of 0.90. Coolant fraction Y is about 0.037 throughout this range.

The efficiency of both configurations (fig. 7(b)) is relatively constant up to an ideal velocity ratio of 0.90. The significant efficiency decrease due to film cooling, already noted at design $\left(V/V_{cr}\right)_{id,3}$ in the discussion of wake shape, persists over the entire range of velocity ratio.

The variation of equivalent coolant flow rate $w_c \sqrt{\theta_{cr}}/\delta$, based on primary-air conditions at the cascade inlet, with coolant to primary-air inlet total-pressure ratio p'_c/p'_1 at design $\left(V/V_{cr}\right)_{id,3}$ for all configurations is shown in figure 8(a). The small-hole configurations (i), (ii), and (iii) agree quite closely. Large-hole configurations (iv) and (vii) are only slightly lower, but large-hole configurations (v), (vi), and (viii) are about 13 percent lower. Also shown are the coolant flow rates for each configuration at a coolant to ambient total-pressure ratio of 1.33 with no primary flow. The proportional positioning agreement between the two indicates that the coolant flow rate variation between configurations is not due to interactions with the primary flow, but is instead due to variations in the internal geometry of the coolant holes.

Coolant flow rate (expressed as a fraction Y of primary flow rate) has very similar positioning (fig. 8(b)), which would be expected when total flow rate is essentially the same for all configurations.

Effect of Hole Size

The effect of hole size on film-cooling losses is shown in figure 9, where configurations (i) and (iv) are compared on the basis of efficiency loss ratio over a range of coolant to primary-air inlet total-pressure ratio at design aftermix ideal critical velocity ratio. In both configurations, the angle of the coolant hole relative to the main-stream flow direction (angle ψ) is zero, and the nominal angle of the hole relative to the local vane surface (angle φ) is 35°. At a coolant total-pressure ratio of 1.0, the efficiency loss ratio for the small-hole configuration (i), which has a nominal hole diameter of 0.0254 centimeter, is 0.71. The loss ratio for the large-hole configuration (iv), which has a nominal hole diameter of 0.0355 centimeter, at the same pressure ratio is 0.66, or 0.05 lower. This difference increases to about 0.10 at a total-pressure ratio of 1.5. A minimum value of efficiency loss ratio occurs at a total-pressure ratio of about 1.05 for each configuration.

Effect of Coolant-Hole Angle Relative to Vane Surface

The effect of the ejection angle, or hole angle, relative to the local vane surface (i.e., angle φ) is shown in figure 10. This figure compares the efficiency loss ratios for small-hole configurations (i), (ii), and (iii), which have all holes orientated in line with the main-stream flow direction ($\psi = 0^{\circ}$). At a coolant total-pressure ratio of 1.0, the efficiency loss ratio for streamwise ejection at an angle of 35° from the vane surface is 0.71. For ejection at 45° from the vane surface, the loss ratio is 0.78, or 0.07 higher. At 55° from the vane surface, however, the loss ratio is 0.93, an increase of 0.22 over the value of 35° ejection. These differences hold relatively constant over the range of coolant total-pressure ratios. Minimum loss values occur at a coolant total-pressure ratio of about 1.05 for all configurations.

Effect of Coolant-Hole Angle Relative to Main-Stream Flow Direction

The effect of ejection at an angle relative to the direction of the main-stream flow as well as at an angle relative to the surface (i.e., compound-angle ejection) is shown in figure 11. This figure compares the efficiency loss ratios for large-hole configurations (iv), (v), and (vii), all with holes oriented at an angle φ of 35° relative to the local vane surface. At a coolant total-pressure ratio of 1.0, the loss ratio for ejection at a 45° angle from the main-stream flow direction (i.e., 45° compound-angle ejection; configuration (v)) is 0.99. This is an increase of 0.33 over the loss ratio of 0.66 for ejection in the direction of the main-stream flow (i.e., streamwise ejection; configuration (iv)).

For ejection at 90° from the direction of the main-stream flow (i.e., spanwise ejection; configuration (vii)), the loss ratio is 1.27. This is 0.61 above the value for streamwise ejection. The loss minimums for 45° compound-angle ejection and for spanwise ejection are considerably more pronounced and occur at higher coolant total-pressure ratios than for streamwise ejection. The minimum loss value for 45° compound-angle ejection is only about 0.07 above the loss ratio of 0.66 for streamwise ejection at the same pressure ratio.

Ejection angles below 35° from the local vane surface are physically obtainable for 45° compound-angle ejection and for spanwise ejection. The effect of ejection at smaller angles with the vane surface is shown in figure 12, which compares configurations (v) and (vi) for 45° compound-angle ejection from large holes, and configurations (vii) and (viii) for spanwise ejection from large holes. For 45° compound-angle ejection, a reduction of the angle from the vane surface φ from 35° to 20° causes a significant decrease (from 0.99 to 0.75) in the efficiency loss ratio at a coolant total-pressure ratio of 1.0. At a pressure ratio of 1.08, the loss ratio is reduced to a value just 0.02 above the value for the minimum-loss configuration (iv). For spanwise ejection, the effect of a reduction of the angle from the vane surface φ from 35° to 15° is small enough to be obscured by the large scatter which was encountered in all spanwise-ejection data.

Comparison of Results for a Coolant Total-Pressure Ratio of 1.0

The ejection geometry effects for coolant ejection from the entire vane surface at a total-pressure ratio of 1.0 are summarized in figure 13. The effects of hole diameter and angle from the vane surface φ are shown in figure 13(a). An increase of the hole diameter from 0.0254 centimeter to 0.0355 centimeter results in a drop of the efficiency loss ratio from 0.71 to 0.66. Increasing the ejection angle from the vane surface φ from 35° to 45° has a relatively minor effect on the efficiency loss ratio, but a further increase to 55° produces a significant loss. The most efficient configuration for streamwise ejection is configuration (iv), which has large holes oriented at a surface angle φ of 35°.

The effect of coolant-hole angle relative to the main-stream flow direction (angle ψ) is summarized in figure 13(b). The efficiency loss ratio for spanwise ejection ($\psi = 90^\circ$) at surface angles of 15° and 35° is about 1.3, or twice as much as for streamwise ejection ($\psi = 0^\circ$). For 45° compound-angle ejection ($\psi = 45^\circ$), the loss ratio is 0.75 at a surface angle φ of 20°, and 0.99 at a surface angle of 35°.

The most efficient configuration tested is configuration (iv), which has large holes oriented in the streamwise direction at a 35° angle from the vane surface. The thermodynamic-efficiency reduction due to film cooling for this minimum-loss configuration is 0.66 percent for each percent of coolant ejected into the primary flow.

Vane Surface Regions

The loss due to cooling in various regions of the vane surface was determined by testing four of the cooling-hole configurations with coolant ejection from individual regions and from combinations of regions of the vane surface. For these tests, the cooling holes in the other regions of the vane surface were filled and leveled to provide a solid, smooth surface. Tested were configuration (iv), with $\psi = 0^{\circ}$ and $\varphi = 35^{\circ}$; configuration (v), $\psi = 45^{\circ}$ and $\varphi = 35^{\circ}$; configuration (vi), with $\psi = 45^{\circ}$ and $\varphi = 20^{\circ}$; and configuration (viii), with $\psi = 90^{\circ}$ and $\varphi = 15^{\circ}$. The vane surface regions (see fig. 2) tested individually were the pressure-surface region, P; the accelerating region of the suction surface, A; the diffusing region of the suction surface, D; and the trailing-edge region, T. The pressure-surface region, the accelerating region of the suction surface, and the trailing-edge region were tested also in combination, PAT. Other combinations tested were the accelerating and diffusing regions of the suction surface, AD, and the diffusing region of the suction surface with the trailing-edge region, DT.

These data were also used to determine whether the coolant flow rates and losses are additive. The coolant flow rate and loss in one region were assumed to be independent of the coolant flow rates and losses in other regions of the vane surface. It was also assumed that the measured loss was composed of the loss of the uncooled (solid) vane and the sum of the losses due to cooling the various regions of the vane.

The total coolant flow rate is

$$w_{c,t} = w_{c,P} + w_{c,A} + w_{c,D} + w_{c,T} \tag{1}$$

and the total loss is

$$\bar{e}_t = \bar{e}_0 + \Delta\bar{e}_P + \Delta\bar{e}_A + \Delta\bar{e}_D + \Delta\bar{e}_T \tag{2}$$

where

$$\bar{e}_t = 1 - \eta$$

and

$$\Delta\bar{e}_i = \eta_0 - \eta_i$$

Equation (2) may be rewritten as

$$\eta_0 - \eta = (\eta_0 - \eta_P) + (\eta_0 - \eta_A) + (\eta_0 - \eta_D) + (\eta_0 - \eta_T) \tag{3}$$

This procedure is compatible with the method of reference 2 provided that the coolant to primary-air inlet total-temperature and total-pressure ratios are each equal to 1.0 and provided that the total (primary plus coolant) flow rate for a given vane is constant in all the tests of the various surface regions. These conditions were very nearly true for all the vanes tested.

All the results presented in this section are for a coolant to primary-air inlet total-pressure ratio (p'_c/p'_1) of 1.0 and for the design aftermix ideal critical velocity ratio.

Loss ratio. - The efficiency loss ratios for three major vane surface regions are shown in figure 14. The largest loss ratios occurred for ejection from the diffusing region of the suction surface. For streamwise ejection, the loss ratio was about 0.9. For 45° compound-angle ejection, the loss ratio increased moderately, to a value of 1.2 to 1.3. For spanwise ejection, the loss ratio increased markedly, to a value of 2.2, which is about $2\frac{1}{2}$ times the value for streamwise ejection.

The loss ratio for the pressure-surface region did not vary greatly with the ejection angle (ψ) relative to the main-stream flow direction. For this region, the loss ratio ranged from about 0.7 for streamwise ejection ($\psi = 0^{\circ}$) to about 0.9 for spanwise ejection ($\psi = 90^{\circ}$). The lowest losses occurred for ejection from the accelerating region of the suction surface. Also, the losses for this region were not very sensitive to ejection angle from streamwise; the loss ratio ranged from about 0.3 for streamwise ejection to 0.2 for spanwise ejection.

Addition of flows and losses. - In figure 15, the sums of the flow rates and the sums of the losses obtained for various individual surface regions and for combinations of regions are compared with the flow rates and the losses obtained with fully cooled vanes. The regional flow-rate totals (fig. 15(a)) agree very closely with the flow rate for the fully cooled vane. The regional loss totals (fig. 15(b)) are in general agreement. For each configuration, two of the three bar graphs are very close, with the third disagreeing by about 0.005.

Flow and loss interactions between regions. - A comparison of flow-rate and loss values (fig. 16) obtained for individual surface regions by subtraction and by direct measurement provides some insight into the interactions between the various regions. Figure 16(a) shows excellent agreement of calculated (by subtraction) and measured values of coolant flow rate. Coolant flow rate from a given region did not appreciably affect the coolant flow rate from any other region.

The comparison of losses (fig. 16(b)) indicates general agreement. However, the losses seem to be affected by an interaction of the coolant flows from the accelerating region and the diffusing region of the suction surface. Unfortunately, because the accelerating region was not tested separately, the coolant losses for this region had to be determined by subtraction. Figure 16(b) shows that for the accelerating region the losses determined by method 1 were always higher than those determined by method 2.

This suggests that the loss for either the accelerating region or the diffusing region alone is larger than the loss for the two regions combined. This is in agreement with the full-film results shown in figure 15(b). With full-film cooling, the sum of the loss for the combined accelerating region, pressure-surface region, and trailing-edge region (APT) plus the loss for the diffusing region (D) alone was always greater than the sum of the loss for the pressure-surface region (P) alone plus the loss for the combined accelerating region and diffusing region (AD) plus the loss for the trailing-edge region (T) alone. One explanation for this is that coolant ejection from the accelerating region may be causing the transition from a laminar to a turbulent boundary layer to occur earlier than it would without ejection from that region. The effect on the loss in the diffusing region would depend on whether there were coolant flow in the accelerating region or the diffusing region or both. Testing of the accelerating region alone is required to define this interaction.

CONCLUDING REMARKS

Film-cooling flow-visualization studies indicate that compound-angle ejection provides better film coverage than does streamwise ejection. A major object of the investigation reported herein was to evaluate the aerodynamic penalty for compound-angle ejection. For coolant ejection from the pressure-surface region and the accelerating (forward) region of the suction surface, it appears that the ejection angle relative to the streamwise direction can be dictated from cooling considerations, with comparatively little effect on the overall vane loss. For the diffusing (aft) region of the suction surface, the effect of the ejection angle from the streamwise direction is larger, and a compromise must be made between cooling performance and aerodynamic loss.

Minimum values of loss ratio occurred at coolant to primary-air inlet total-pressure ratios above 1.0 for all configurations and all regions. For compound-angle ejection, these minimums were quite pronounced, making the loss comparison with streamwise ejection more favorable. This would be a definite factor in a consideration of film cooling for second-stage blading.

SUMMARY OF RESULTS

The effect of film-cooling hole geometry on the aerodynamic performance of a turbine vane was measured in a two-dimensional cascade. Nominal hole diameters of 0.0254 and 0.0356 centimeter and nominal hole orientations of 35°, 45°, and 55° from the local vane surface and 0°, 45°, and 90° from the main-stream flow direction were investigated. In addition, the contribution of individual regions of the vane surface to the overall effect was determined. Ambient-temperature air was used for both cascade and coolant. Tests were made over a range of aftermix ideal critical velocity ratio from 0.6 to 0.94 at a coolant to primary-air inlet total-pressure ratio of 1.0, and over a range of coolant to primary-air inlet total-pressure ratio from 1.0 to 1.5 at an aftermix ideal critical velocity ratio of 0.81. The principal measurements were surveys of total pressure, static pressure, and flow angle downstream from the vane exit. Loss results are expressed in terms of percent decrease in thermodynamic efficiency of the test vane below the value for an uncooled (solid) vane per percent coolant ejected, or loss ratio. This summary is limited to results for a coolant to primary-air inlet total-pressure ratio of 1.0, as this is a realistic design condition for vanes. The following are the principal results of the investigation:

1. For coolant ejection from the pressure-surface region or from the accelerating (forward) region of the suction surface, the loss ratio is fairly insensitive to the angle of ejection relative to the main-stream flow direction. For an angle change from 0° to 90°, the loss ratio varied from 0.7 to 0.9 for ejection from the pressure-surface region, and from 0.3 to 0.2 for ejection from the accelerating region. For 45° compound-angle ejection from these same regions of the vane surface, a reduction of the ejection angle relative to the local vane surface from 35° to 20° also had very little effect on the loss ratio.

2. For coolant ejection from the diffusing (aft) region of the suction surface, the loss ratio is high and very sensitive to the angle of ejection relative to the main-stream flow direction. The loss ratio increased from 0.9 for streamwise ejection to 1.3 for 45° compound-angle ejection and to 2.2 for spanwise ejection. With 45° compound-angle ejection, a reduction of the surface angle from 35° to 20° resulted in a decrease in loss ratio from 1.3 to 1.2. The loss ratio for streamwise ejection from the diffusing region (0.9) is higher than for the pressure-surface region (0.7) and much higher than for the accelerating region (0.2).

3. For coolant ejection from the entire vane surface (all regions), the loss ratio is lowest for streamwise ejection from large holes at an angle of 35° with the local surface. Efficiency decreased 0.66 percent for each percent of coolant flow. The loss ratio is fairly sensitive to the angle of ejection relative to the main-stream flow direction. The loss ratio increased to 1.0 for 45° compound-angle ejection and to 1.3 for spanwise ejection. Reducing the ejection angle relative to the vane surface from 35° to 20° for 45° compound-angle ejection reduced the loss ratio to 0.76, which compares favorably with the value of 0.66 for streamwise ejection.

4. For coolant ejection from the entire vane surface, the loss ratio is somewhat less for larger diameter holes. Increasing the hole diameter from 0.0254 centimeter to 0.0356 centimeter resulted in a decrease in loss ratio from 0.76 to 0.66.

5. Coolant flow rates for ejection from individual regions can be added to very closely predict flow rates for ejection from the entire vane surface (all regions). Cooling losses for ejection from individual regions can be added to predict, in general, losses for ejection from the entire vane surface. The maximum error for two independent loss summations for each of four configurations was about 0.005 of the efficiency of the solid vane.

Lewis Research Center,
National Aeronautics and Space Administration,
Cleveland, Ohio, September 27, 1977,
505-04.

REFERENCES

1. Moffitt, Thomas P.; Prust, Herman W., Jr.; Szanca, Edward M.; and Schum, Harold J.: Summary of Cold-Air Tests of a Single-Stage Turbine with Various Stator Cooling Techniques. NASA TM X-52968, 1971.

2. Moffitt, Thomas P.; Prust, Herman W., Jr.; and Bartlett, Wayne M.: Two-Dimensional Cold-Air Cascade Study of a Film-Cooled Turbine Stator Blade. I - Experimental Results of Pressure-Surface Film Cooling Tests. NASA TM X-3045, 1974.

3. Prust, Herman W., Jr.: Two-Dimensional Cold-Air Cascade Study of a Film-Cooled Turbine Stator Blade. II - Experimental Results of Full Film Cooling Tests. NASA TM X-3153, 1975.

4. Prust, Herman W., Jr.; and Moffitt, Thomas P.: Two-Dimensional Cold-Air Cascade Study of a Film-Cooled Turbine Stator Blade. III - Effect of Hole Size on Single-Row and Multi-Row Ejection. NASA TM X-3442, 1976.

5. Colladay, R. S.; and Russell, L. M.: Streakline Flow Visualization of Discrete Hole Film Cooling for Gas Turbine Applications. J. Heat Trans., vol. 98, ser. C., no. 2, May 1976, pp. 245-250.

6. Szanca, Edward M.; Schum, Harold J.; and Hotz, Glen M.: Research Turbine for High-Temperature Core Engine Application. I - Cold-Air Overall Performance of Solid Scaled Turbine. NASA TN D-7557, 1974.

7. McDonel, J. D.; Hsia, E. S.; and Hartzel, J. E.: Core Turbine Aerodynamic Evaluation: Design of Initial Turbine. NASA CR-2512, 1975.

8. Kline, John J.; and Stabe, Roy G.: Two-Dimensional Cascade Test of a Highly Loaded, Low-Solidity, Tandem Airfoil Turbine Rotor Blade. NASA TM X-2729, 1973.

9. Stabe, Roy G.; and Kline, John F.: Aerodynamic Performance of a Fully Film Cooled Core Turbine Vane Tested with Cold Air in a Two-Dimensional Cascade. NASA TM X-3177, 1975.

10. Goldman, Louis J.; and McLallin, Kerry L.: Cold-Air Annular-Cascade Investigation of Aerodynamic Performance of Cooled Turbine Vanes. I - Facility Description and Base (Solid) Vane Performance. NASA TM X-3006, 1974.

TABLE I. - COOLING HOLE GEOMETRY

(a) Small-hole configurations

Vane surface region	Hole row	Number of holes	Hole diameter, cm	Hole spacing, cm	Configuration (i): Relative to local vane surface, φ	Configuration (i): Relative to main-stream flow direction, ψ	Configuration (ii): Relative to local vane surface, φ	Configuration (ii): Relative to main-stream flow direction, ψ	Configuration (iii): Relative to local vane surface, φ	Configuration (iii): Relative to main-stream flow direction, ψ
					Coolant ejection angles, φ and ψ, deg					
Suction surface:										
Accelerating region, A	1	61	0.0343	0.127	90	0	90	0	90	0
	2	60	.0343	.127	44	↓	44	↓	45	↓
	3	31	.0254	.254	44	↓	54	↓	64	↓
	4	30	↓	↓	45	↓	55	↓	65	↓
	5	31	↓	↓	35	↓	45	↓	55	↓
	6	30	↓	↓	35	↓	45	↓	55	↓
	7	31	↓	↓	35	↓	45	↓	55	↓
Diffusing region, D	8	30	0.0254	0.254	35	0	45	0	55	0
	9	31	↓	↓	↓	↓	↓	↓	↓	↓
	10	30	↓	↓	↓	↓	↓	↓	↓	↓
	11	31	↓	↓	↓	↓	↓	↓	↓	↓
	12	30	↓	↓	↓	↓	↓	↓	↓	↓
	13	31	↓	↓	↓	↓	↓	↓	↓	↓
	14	30	↓	↓	↓	↓	↓	↓	↓	↓
	15	31	↓	↓	↓	↓	↓	↓	↓	↓
	16	30	↓	↓	↓	↓	↓	↓	↓	↓
	17	31	↓	↓	↓	↓	↓	↓	↓	↓
	18	30	↓	↓	↓	↓	↓	↓	↓	↓
	19	31	↓	↓	↓	↓	↓	↓	↓	↓
	20	30	↓	↓	↓	↓	↓	↓	↓	↓
	21	31	↓	↓	↓	↓	↓	↓	↓	↓
	22	30	↓	↓	↓	↓	↓	↓	↓	↓
	23	31	↓	↓	↓	↓	↓	↓	↓	↓
	24	30	↓	↓	↓	↓	↓	↓	↓	↓
Trailing-edge region, T	25	60	0.0254	0.127	90	0	90	0	90	0
Pressure-surface region, P	26	31	0.0254	0.254	35	0	42	0	52	0
	27	30	↓	↓	↓	↓	45	↓	55	↓
	28	31	↓	↓	↓	↓	↓	↓	↓	↓
	29	30	↓	↓	↓	↓	↓	↓	↓	↓
	30	31	↓	↓	↓	↓	↓	↓	↓	↓
	31	30	↓	↓	↓	↓	↓	↓	↓	↓
	32	31	↓	↓	↓	↓	↓	↓	↓	↓
	33	30	↓	↓	↓	↓	↓	↓	↓	↓
	34	31	↓	↓	↓	↓	↓	↓	↓	↓
	35	30	↓	↓	↓	↓	↓	↓	↓	↓
	36	31	↓	↓	↓	↓	↓	↓	↓	↓
	37	30	↓	↓	↓	↓	↓	↓	↓	↓
	38	31	↓	↓	↓	↓	↓	↓	↓	↓
	39	30	↓	↓	↓	↓	↓	↓	↓	↓
	40	31	↓	↓	↓	↓	↓	↓	↓	↓
	41	30	↓	↓	↓	↓	↓	↓	↓	↓
	42	31	↓	↓	↓	↓	↓	↓	↓	↓
	43	30	↓	↓	↓	↓	↓	↓	↓	↓
	44	31	↓	↓	44	↓	↓	↓	↓	↓
	45	60	0.0343	0.127	45	↓	↓	↓	↓	↓

TABLE I. - Concluded.

(b) Large-hole configurations

Vane surface region	Hole row	Number of holes	Hole diameter, cm	Hole spacing, cm	Configuration (iv): Relative to local vane surface, φ	(iv): Relative to main-stream flow direction, ψ	(v): Relative to local vane surface, φ	(v): Relative to main-stream flow direction, ψ	(vi): Relative to local vane surface, φ	(vi): Relative to main-stream flow direction, ψ	(vii): Relative to local vane surface, φ	(vii): Relative to main-stream flow direction, ψ	(viii): Relative to local vane surface, φ	(viii): Relative to main-stream flow direction, ψ
					Coolant ejection angles, φ and ψ, deg									
Suction surface:														
Accelerating region, A	1	31	0.0483	0.254	90	0	35	90	20	90	35	90	15	90
	2	30	.0483	.254	44	↓	40	45	40	45	↓	↓	↓	↓
	3	16	.0356	.508	44	↓	35	↓	30	↓	↓	↓	↓	↓
	4	15	↓	↓	45	↓	↓	↓	28	↓	↓	↓	↓	↓
	5	16	↓	↓	35	↓	↓	↓	27	↓	↓	↓	↓	↓
	6	15	↓	↓	35	↓	↓	↓	25	↓	↓	↓	↓	↓
	7	16	↓	↓	35	↓	↓	↓	25	↓	↓	↓	↓	↓
Diffusing region, D	8	15	0.0356	0.508	35	0	35	45	25	45	35	90	15	90
	9	16	↓	↓	↓	↓	↓	↓	24	↓	↓	↓	↓	↓
	10	15	↓	↓	↓	↓	↓	↓	22	↓	↓	↓	↓	↓
	11	16	↓	↓	↓	↓	↓	↓	20	↓	↓	↓	↓	↓
	12	15	↓	↓	↓	↓	↓	↓	↓	↓	↓	↓	↓	↓
	13	16	↓	↓	↓	↓	↓	↓	↓	↓	↓	↓	↓	↓
	14	15	↓	↓	↓	↓	↓	↓	↓	↓	↓	↓	↓	↓
	15	16	↓	↓	↓	↓	↓	↓	↓	↓	↓	↓	↓	↓
	16	15	↓	↓	↓	↓	↓	↓	↓	↓	↓	↓	↓	↓
	17	16	↓	↓	↓	↓	↓	↓	↓	↓	↓	↓	↓	↓
	18	15	↓	↓	↓	↓	↓	↓	↓	↓	↓	↓	↓	↓
	19	16	↓	↓	↓	↓	↓	↓	↓	↓	↓	↓	↓	↓
	20	15	↓	↓	↓	↓	↓	↓	↓	↓	↓	↓	↓	↓
	21	16	↓	↓	↓	↓	↓	↓	↓	↓	↓	↓	↓	↓
	22	15	↓	↓	↓	↓	↓	↓	↓	↓	↓	↓	↓	↓
	23	16	↓	↓	↓	↓	↓	↓	↓	↓	↓	↓	↓	↓
	24	15	↓	↓	↓	↓	↓	↓	↓	↓	↓	↓	↓	↓
Trailing-edge region, T	25	30	0.0356	0.254	90	0	90	0	90	0	90	0	90	0
Pressure-surface region, P	26	16	0.0356	0.508	35	0	35	45	20	45	35	90	15	90
	27	15	↓	↓	↓	↓	↓	↓	↓	↓	↓	↓	↓	↓
	28	16	↓	↓	↓	↓	↓	↓	↓	↓	↓	↓	↓	↓
	29	16	↓	↓	↓	↓	↓	↓	↓	↓	↓	↓	↓	↓
	30	16	↓	↓	↓	↓	↓	↓	↓	↓	↓	↓	↓	↓
	31	15	↓	↓	↓	↓	↓	↓	↓	↓	↓	↓	↓	↓
	32	16	↓	↓	↓	↓	↓	↓	↓	↓	↓	↓	↓	↓
	33	15	↓	↓	↓	↓	↓	↓	↓	↓	↓	↓	↓	↓
	34	16	↓	↓	↓	↓	↓	↓	↓	↓	↓	↓	↓	↓
	35	15	↓	↓	↓	↓	↓	↓	↓	↓	↓	↓	↓	↓
	36	16	↓	↓	↓	↓	↓	↓	↓	↓	↓	↓	↓	↓
	37	15	↓	↓	↓	↓	↓	↓	↓	↓	↓	↓	↓	↓
	38	16	↓	↓	↓	↓	↓	↓	↓	↓	↓	↓	↓	↓
	39	15	↓	↓	↓	↓	↓	↓	↓	↓	↓	↓	↓	↓
	40	16	↓	↓	↓	↓	↓	↓	↓	↓	↓	↓	↓	↓
	41	15	↓	↓	↓	↓	↓	↓	↓	↓	↓	↓	↓	↓
	42	16	↓	↓	↓	↓	↓	↓	↓	↓	↓	↓	↓	↓
	43	15	↓	↓	↓	↓	↓	↓	22	↓	↓	↓	↓	↓
	44	16	↓	↓	44	↓	42	↓	42	↓	↓	↓	↓	↓
	45	30	0.0483	0.254	45	↓	42	↓	42	↓	↓	↓	↓	↓

TABLE II. - TURBINE-VANE FILM-COOLING TEST DATA

Configuration	Vane surface region	Velocity ratio, $(V/V_{cr})_{id,3}$	Coolant pressure ratio, p'_c/p'_1	Coolant fraction, Y	Efficiency, η	Equivalent primary flow rate, $w_p\sqrt{\theta_{cr}}/\delta$, (g/sec)/cm	Exit flow angle, α_3, deg	Equivalent coolant flow rate, $w_c\sqrt{\theta_{cr}}/\delta$, (g/sec)/cm	Efficiency loss fraction, $(\eta_0 - \eta)/\eta_0$	Efficiency loss ratio, $(\eta_0 - \eta)/\eta_0 Y$
Solid		0.592	-----	------	0.9788	30.93	67.2	-----	------	-----
		.644	-----	------	.9782	32.27	67.3	-----	------	-----
		.693	-----	------	.9788	33.88	67.3	-----	------	-----
		.738	-----	------	.9791	35.06	67.3	-----	------	-----
		.802	-----	------	.9791	36.47	67.1	-----	------	-----
		.802	-----	------	.9792	36.63	67.2	-----	------	-----
		.836	-----	------	.9783	37.00	67.2	-----	------	-----
		.890	-----	------	.9759	37.39	67.4	-----	------	-----
		.914	-----	------	.9740	37.77	67.3	-----	------	-----
		.931	-----	------	.9697	38.02	67.0	-----	------	-----
(i)	PADT	0	1.335	------	------	-----	----	2.261	------	-----
		.818	1.001	0.0396	0.9503	34.16	67.6	1.354	0.0281	0.710
		.820	1.002	.0402	.9510	33.95	67.7	1.363	.0286	.711
		.818	1.053	.0483	.9461	33.73	67.7	1.629	.0336	.696
		.818	1.101	.0543	.9414	33.66	67.7	1.829	.0384	.707
		.818	1.201	.0660	.9303	33.16	67.7	2.189	.0497	.754
		.817	1.302	.0761	.9191	32.89	67.7	2.505	.0612	.804
		.817	1.403	.0863	.9066	32.41	67.8	2.797	.0740	.857
		.819	1.501	.0943	.8951	32.50	67.7	3.064	.0857	.909
		.819	1.501	.0931	.8956	32.73	67.7	3.047	.0852	.915

(ii)	PADT	0	1.330	------	------	-----	----	2.261	------	-----
		.816	.999	0.0391	0.9490	34.61	67.2	1.354	0.0306	0.784
		.818	1.000	.0397	.9486	34.29	67.4	1.359	.0311	.782
		.814	1.049	.0473	.9454	34.20	67.3	1.618	.0343	.726
		.814	1.100	.0542	.9394	33.89	67.4	1.836	.0404	.746
		.818	1.195	.0647	.9276	33.63	67.4	2.177	.0525	.811
		.817	1.197	.0648	.9269	33.70	67.3	2.182	.0532	.821
		.813	1.296	.0753	.9146	33.13	67.5	2.495	.0658	.874
		.818	1.303	.0755	.9147	33.27	67.3	2.511	.0657	.870
		.818	1.398	.0839	.9033	33.18	67.4	2.784	.0773	.922
		.816	1.504	.0939	.8881	32.70	67.5	3.070	.0928	.989
(iii)	PADT	0	1.328	------	------	-----	----	2.275	------	-----
		.810	1.001	0.0407	0.9411	33.79	67.6	1.375	0.0387	0.951
		.814	1.001	.0411	.9423	33.57	67.7	1.380	.0375	.912
		.814	1.050	.0493	.9366	33.34	67.7	1.643	.0433	.878
		.814	1.098	.0557	.9299	33.06	67.8	1.841	.0502	.900
		.814	1.202	.0674	.9171	32.79	67.7	2.209	.0632	.938
		.814	1.298	.0770	.9035	32.56	67.7	2.505	.0771	1.002
		.813	1.398	.0860	.8897	32.39	67.7	2.788	.0912	1.061
		.814	1.500	.0959	.8750	31.88	67.8	3.059	.1062	1.108
(iv)	AD	0	1.330	------	------	-----	----	1.227	------	-----
		[a].800	[a].999	[a]0.0262	[a]0.9617	[a]32.82	[a]68.8	[a].861	[a]0.0177	[a]0.674
		.803	1.000	.0263	.9608	32.81	68.7	.864	.0186	.707
		.803	1.048	.0301	.9585	32.64	68.7	.982	------	-----
		.803	1.096	.0329	.9543	32.68	68.7	1.075	------	-----
		.803	1.198	.0383	.9476	32.47	68.6	1.245	------	-----
		.807	1.299	.0429	.9421	32.43	68.7	1.393	------	-----
		.807	1.398	.0466	.9365	32.81	68.6	1.529	------	-----
		.807	1.493	.0510	.9301	32.57	68.6	1.661	------	-----
		.800	1.495	.0515	.9285	32.14	68.8	1.655	------	-----
		.804	1.500	.0514	.9293	32.31	68.8	1.661	------	-----

[a]Data set used for regional flow-rate and loss comparisons.

TABLE II. - Continued.

Configuration	Vane surface region	Velocity ratio, $(V/V_{cr})_{id,3}$	Coolant pressure ratio, p'_c/p'_1	Coolant fraction, Y	Efficiency, η	Equivalent primary flow rate, $w_p\sqrt{\theta_{cr}}/\delta$, (g/sec)/cm	Exit flow angle, α_3, deg	Equivalent coolant flow rate, $w_c\sqrt{\theta_{cr}}/\delta$, (g/sec)/cm	Efficiency loss fraction, $(\eta_0 - \eta)/\eta_0$	Efficiency loss ratio, $(\eta_0 - \eta)/\eta_0 Y$
(iv)	D	0	1.333	------	------	-----	----	0.702	------	------
		.814	.995	0.0169	0.9627	34.48	68.0	.584	0.0166	0.985
		.814	.997	.0170	.9633	34.63	67.9	.589	.0160	.743
		.809	.704	.0067	.9707	34.64	68.0	.232	------	-----
		.812	.795	.0108	.9683	34.77	68.0	.373	------	-----
		.812	.900	.0142	.9669	34.66	67.9	.491	------	-----
		.815	1.048	.0182	.9618	34.23	68.0	.625	------	-----
		.815	1.100	.0195	.9605	34.57	68.0	.673	------	-----
		.817	1.205	.0221	.9580	34.45	68.0	.761	------	-----
		.817	1.296	.0237	.9553	34.64	67.9	.821	------	-----
		.820	1.396	.0256	.9530	35.43	67.4	.907	------	-----
		.821	1.495	.0279	.9486	35.07	67.5	.979	------	-----
(iv)	D	0	1.332	------	------	-----	----	0.725	------	-----
		[a].801	[a].999	[a]0.0179	[a]0.9638	[a]33.43	[a]68.6	[a].600	[a]0.0155	[a]0.867
		.803	1.001	.0181	.9637	33.32	68.5	.602	.0156	.863
		.799	1.050	.0192	.9621	33.64	68.5	.646	------	-----
		.804	1.100	.0207	.9598	33.39	68.5	.691	------	-----
		.803	1.204	.0234	.9572	33.22	68.6	.779	------	-----
		.809	1.300	.0258	.9544	33.22	68.6	.855	------	-----
		.810	1.402	.0280	.9506	33.29	68.6	.932	------	-----
		.809	1.503	.0300	.9460	33.56	68.6	1.009	------	-----

(iv)	DT	0	1.333	------	------	-----	----	0.771	------	-----
		.818	.999	0.0180	0.9619	35.61	67.3	.641	0.0175	0.970
		.818	.999	.0180	.9622	35.63	67.2	.641	.0172	.953
		.819	1.049	.0193	.9611	35.77	67.2	.689	------	-----
		.815	1.098	.0207	.9580	35.59	67.2	.736	------	-----
		.818	1.199	.0232	.9552	35.54	67.2	.825	------	-----
		.818	1.301	.0257	.9521	35.57	67.2	.913	------	-----
		.819	1.397	.0279	.9490	35.50	67.2	.991	------	-----
		.819	1.464	.0295	.9484	35.45	67.2	1.045	------	-----
(iv)	DT	0	1.328	------	------	-----	----	0.748	------	-----
		[a].802	[a].997	[a]0.0184	[a]0.9642	[a]33.63	[a]68.5	[a].618	[a]0.0151	[a]0.822
		.803	1.000	.0183	.9637	33.88	68.4	.620	.0156	.854
		.807	.997	.0182	.9638	33.84	68.4	.614	.0155	.853
		.802	.724	.0075	.9706	34.23	68.4	.257	------	-----
		.803	.796	.0111	.9702	34.18	68.3	.379	------	-----
		.806	.897	.0148	.9684	34.16	68.4	.505	------	-----
		.807	1.051	.0195	.9627	33.77	68.4	.659	------	-----
		.811	1.099	.0207	.9605	33.80	68.4	.698	------	-----
		.811	1.206	.0235	.9568	33.77	68.4	.793	------	-----
		.810	1.301	.0261	.9555	33.63	68.5	.877	------	-----
		.811	1.404	.0285	.9496	33.84	68.4	.964	------	-----
		.810	1.495	.0312	.9450	33.39	68.4	1.036	------	-----
		.806	.997	.0182	.9643	33.91	68.4	.618	------	-----
(iv)	P	0	1.333	------	------	-----	----	0.970	------	-----
		[a].797	[a].999	[a]0.0108	[a]0.9716	[a]35.93	[a]67.2	[a].389	[a]0.0076	[a]0.700
		.800	.999	.0109	.9714	35.66	67.2	.389	.0078	.712
		.797	1.049	.0152	.9704	35.50	67.3	.541	------	-----
		.797	1.100	.0188	.9691	35.47	67.3	.664	------	-----
		.798	1.200	.0241	.9652	35.29	67.3	.850	------	-----
		.798	1.301	.0285	.9611	35.20	67.2	1.005	------	-----
		.797	1.406	.0322	.9572	35.22	67.2	1.136	------	-----
		.797	1.500	.0359	.9525	35.11	67.3	1.263	------	-----

[a]Data set used for regional flow-rate and loss comparisons.

TABLE II. - Continued.

Configuration	Vane surface region	Velocity ratio, $(V/V_{cr})_{id,3}$	Coolant pressure ratio, p_c'/p_1'	Coolant fraction, Y	Efficiency, η	Equivalent primary flow rate, $w_p\sqrt{\theta_{cr}}/\delta$, (g/sec)/cm	Exit flow angle, α_3, deg	Equivalent coolant flow rate, $w_c\sqrt{\theta_{cr}}/\delta$, (g/sec)/cm	Efficiency loss fraction, $(\eta_0 - \eta)/\eta_0$	Efficiency loss ratio, $(\eta_0 - \eta)/\eta_0 Y$
(iv)	PAT	0	1.331	------	------	-----	-----	1.491	------	-----
		[a].811	[a]1.002	[a]0.0210	[a]0.9649	[a]34.00	[a]68.4	[a].713	[a]0.0144	[a]0.686
		.814	.998	.0204	.9659	33.95	68.3	.693	.0134	.656
		.815	1.051	.0274	.9633	33.75	68.3	.925	------	-----
		.815	1.101	.0325	.9600	33.52	68.4	1.089	------	-----
		.818	1.203	.0407	.9538	33.41	68.4	1.359	------	-----
		.819	1.301	.0477	.9471	33.13	68.4	1.582	------	-----
		.822	1.370	.0519	.9421	33.16	68.4	1.721	------	-----
		.822	1.498	.0597	.9298	33.93	68.3	1.964	------	-----
(iv)	PADT	0	1.328	------	------	-----	-----	2.268	------	-----
		.808	1.001	0.0410	0.9555	32.98	68.3	1.354	0.0240	0.585
		.809	1.002	.0412	.9560	32.91	68.3	1.357	.0235	.570
		.813	1.002	.0410	.9555	33.13	68.3	1.357	.0240	.585
		.816	1.046	.0482	.9519	33.20	68.2	1.600	------	-----
		.816	1.102	.0561	.9462	32.77	68.2	1.839	------	-----
		.822	1.178	.0651	.9395	32.61	68.2	2.122	------	-----
		.822	1.202	.0673	.9374	32.77	68.1	2.205	------	-----
		.823	1.283	.0756	.9298	32.54	68.2	2.459	------	-----
		.823	1.392	.0856	.9203	32.43	68.1	2.775	------	-----
		.829	1.499	.0948	.9101	32.38	68.0	3.068	------	-----
		.818	.998	.0400	.9574	33.48	68.2	1.339	.0221	.552

(iv)	PADT	0	1.330	------	------	-----	----	2.229	------	-----
		.605	.999	0.0372	0.9517	29.59	67.3	1.102	------	-----
		.659	1.000	.0375	.9512	31.38	67.3	1.177	------	-----
		.715	1.000	.0371	.9532	33.00	67.1	1.227	------	-----
		.763	1.001	.0376	.9543	34.06	67.1	1.279	------	-----
		.812	.999	.0369	.9551	35.38	66.8	1.307	0.0244	0.662
		.856	.999	.0371	.9567	36.02	66.8	1.336	------	-----
		.900	1.000	.0372	.9575	36.61	66.6	1.364	------	-----
		.939	.999	.0371	.9480	37.27	66.3	1.384	------	-----
		[a].811	[a].999	[a].0376	[a].9545	[a]34.77	[a]67.2	[a]1.309	[a].0250	[a].666
		.811	1.050	.0462	.9500	34.20	67.3	1.580	.0296	.641
		.812	1.099	.0522	.9458	34.31	67.3	1.789	.0339	.650
		.812	1.200	.0632	.9363	33.91	67.3	2.145	.0436	.690
		.811	1.297	.0726	.9267	33.64	67.3	2.443	.0534	.736
		.814	1.400	.0821	.9168	33.31	67.4	2.736	.0635	.774
		.814	1.502	.0902	.9077	33.32	67.4	3.007	.0728	.807
(v)	AD	0	1.330	------	------	-----	----	1.059	------	-----
		[a].820	[a].998	[a]0.0211	[a]0.9586	[a]35.61	[a]67.2	[a].752	[a]0.0208	[a]0.988
		.817	1.006	.0216	.9575	35.54	67.1	.768	.0220	1.017
		.820	1.050	.0242	.9551	35.22	67.2	.854	------	-----
		.819	1.100	.0267	.9519	35.11	67.2	.938	------	-----
		.819	1.203	.0308	.9479	35.32	67.2	1.089	------	-----
		.819	1.302	.0347	.9398	35.18	67.1	1.220	------	-----
		.819	1.404	.0386	.9295	34.93	67.1	1.346	------	-----
		.819	1.499	.0420	.9216	34.81	67.2	1.461	------	-----

[a]Data set used for regional flow-rate and loss comparisons.

TABLE II. - Continued.

Configuration	Vane surface region	Velocity ratio, $(V/V_{cr})_{id,3}$	Coolant pressure ratio, p'_c/p'_1	Coolant fraction, Y	Efficiency, η	Equivalent primary flow rate, $w_p \sqrt{\theta_{cr}}/\delta$, (g/sec)/cm	Exit flow angle, α_3, deg	Equivalent coolant flow rate, $w_c \sqrt{\theta_{cr}}/\delta$, (g/sec)/cm	Efficiency loss fraction, $(\eta_0 - \eta)/\eta_0$	Efficiency loss ratio, $(\eta_0 - \eta)/\eta_0 Y$
(v)	D	0	1.323	------	------	-----	----	0.584	------	-----
		[a].798	[a]1.001	[a]0.0147	[a]0.9602	[a]33.71	[a]68.3	[a].495	[a]0.0192	[a]1.306
		.839	.997	.0147	.9611	34.34	68.3	.504	.0183	1.244
		.798	1.000	.0147	.9601	33.66	68.4	.495	.0193	1.313
		.797	1.052	.0159	.9579	33.70	68.4	.536	------	-----
		.797	1.086	.0166	.9578	33.73	68.3	.561	------	-----
		.800	1.204	.0192	.9527	33.52	68.3	.643	------	-----
		.804	1.306	.0213	.9487	33.32	68.4	.711	------	-----
		.803	1.403	.0231	.9437	33.34	68.5	.771	------	-----
		.804	1.495	.0250	.9390	33.16	68.5	.830	------	-----
(v)	DT	0	1.326	------	------	-----	----	0.630	------	-----
		[a].801	[a].999	[a]0.0157	[a]0.9605	[a]33.84	[a]68.3	[a].530	[a]0.0189	[a]1.204
		.799	.728	.0065	.9720	34.50	68.3	.225	------	-----
		.799	.799	.0095	.9693	34.32	68.3	.327	------	-----
		.804	.895	.0129	.9640	33.72	68.3	.436	------	-----
		.805	.999	.0155	.9604	34.16	68.2	.530	.0190	1.226
		.802	1.048	.0169	.9586	33.75	68.2	.571	------	-----
		.803	1.100	.0182	.9555	33.68	68.3	.611	------	-----
		.802	1.203	.0205	.9515	33.70	68.2	.689	------	-----
		.802	1.298	.0223	.9495	33.93	68.3	.757	------	-----
		.805	1.397	.0243	.9425	33.97	68.2	.825	------	-----
		.806	1.500	.0265	.9367	33.57	68.1	.891	------	-----

(v)	P	0	1.329	------	------	-----	----	0.880	------	-----
		[a].810	[a].996	[a]0.0099	[a]0.9723	[a]35.13	[a]67.7	[a].348	[a]0.0068	[a]0.691
		.814	.997	.0099	.9726	35.43	67.7	.350	.0065	.660
		.815	1.053	.0145	.9694	35.16	67.8	.511	------	-----
		.815	1.097	.0171	.9677	35.09	67.8	.598	------	-----
		.815	1.199	.0223	.9586	34.81	67.9	.777	------	-----
		.816	1.298	.0264	.9516	34.57	67.8	.913	------	-----
		.816	1.396	.0298	.9517	34.77	67.7	1.038	------	-----
		.815	1.498	.0336	.9478	34.41	67.8	1.157	------	-----
(v)	PAT	0	1.329	------	------	-----	----	1.421	------	-----
		.813	1.002	0.0202	0.9687	34.05	68.5	.688	0.0105	0.521
		[a].813	[a]1.001	[a].0199	[a].9681	[a]34.29	[a]68.1	[a].684	[a].0111	[a].559
		.814	1.053	.0266	.9617	33.82	68.1	.900	------	-----
		.811	1.102	.0309	.9570	33.91	68.0	1.046	------	-----
		.812	1.200	.0387	.9492	33.54	68.1	1.298	------	-----
		.811	1.300	.0461	.9372	32.84	68.4	1.513	------	-----
		.811	1.410	.0517	.9303	33.36	68.0	1.725	------	-----
		.807	1.476	.0550	.9282	33.45	68.0	1.841	------	-----
(v)	PADT	0	1.333	------	------	-----	----	2.055	------	-----
		.824	1.001	0.0363	0.9432	33.45	68.1	1.216	0.0366	1.007
		[a].824	[a]1.001	[a].0362	[a].9444	[a]33.63	[a]68.1	[a]1.218	[a].0353	[a].976
		.824	1.055	.0440	.9450	33.64	67.9	1.482	.0347	.789
		.823	1.106	.0502	.9439	33.36	68.0	1.673	.0359	.714
		.828	1.202	.0608	.9320	32.70	68.2	1.988	.0480	.790
		.828	1.304	.0671	.9258	33.89	67.5	2.275	.0543	.810
		.829	1.405	.0773	.9109	32.73	67.9	2.532	.0696	.900
		.830	1.503	.0875	.8975	31.70	68.5	2.773	.0832	.951

[a]Data set used for regional flow-rate and loss comparisons.

TABLE II. - Continued.

Configuration	Vane surface region	Velocity ratio, $(V/V_{cr})_{id,3}$	Coolant pressure ratio, p_c'/p_1'	Coolant fraction, Y	Efficiency, η	Equivalent primary flow rate, $w_p\sqrt{\theta_{cr}}/\delta$, (g/sec)/cm	Exit flow angle, α_3, deg	Equivalent coolant flow rate, $w_c\sqrt{\theta_{cr}}/\delta$, (g/sec)/cm	Efficiency loss fraction, $(\eta_0 - \eta)/\eta_0$	Efficiency loss ratio, $(\eta_0 - \eta)/\eta_0 Y$
(vi)	AD	0	1.327	------	------	-----	----	1.068	------	-----
		[a].822	[a]1.000	[a]0.0216	[a]0.9603	[a]35.61	[a]67.2	[a].770	[a]0.0191	[a]0.884
		.822	1.000	.0217	.9590	35.59	67.1	.771	.0204	.941
		.822	1.052	.0249	.9562	35.25	67.3	.877	------	-----
		.821	1.100	.0274	.9534	35.11	67.3	.961	------	-----
		.817	1.202	.0316	.9480	35.05	67.3	1.109	------	-----
		.818	1.306	.0358	.9429	34.98	67.2	1.254	------	-----
		.821	1.399	..0394	.9376	34.82	67.3	1.371	------	-----
		.816	1.507	.0433	.9297	34.75	67.3	1.505	------	-----
(vi)	D	0	1.331	------	------	-----	----	0.598	------	-----
		.816	1.001	0.0142	0.9630	35.82	67.2	.509	0.0163	1.151
		[a].818	[a]1.002	[a].0143	[a].9621	[a]35.75	[a]67.2	[a].509	[a].0173	[a]1.207
		.818	1.044	.0151	.9623	36.05	67.2	.543	------	-----
		.818	1.102	.0163	.9610	35.89	67.3	.586	------	-----
		.818	1.203	.0183	.9565	35.88	67.3	.657	------	-----
		.818	1.299	.0202	.9507	35.70	67.3	.721	------	-----
		.818	1.399	.0220	.9468	35.70	67.3	.786	------	-----
		.818	1.502	.0242	.9453	35.25	67.3	.852	------	-----

(vi)	DT	0	1.330	------	------	-----	----	0.661	------	-----
		.822	1.001	0.0158	0.9642	35.98	67.0	.570	0.0151	0.957
		.819	.749	.0081	.9691	36.14	67.2	.293	------	-----
		.820	.896	.0131	.9646	35.97	67.2	.470	------	-----
		[a].820	[a]1.003	[a].0160	[a].9634	[a]35.73	[a]67.2	[a].570	[a].0159	[a].996
		.823	1.052	.0171	.9630	35.82	67.2	.614	------	-----
		.819	1.097	.0182	.9604	35.68	67.2	..650	------	-----
		.820	1.201	.0209	.9534	35.05	67.4	.734	------	-----
		.815	1.300	.0231	.9473	34.97	67.5	.809	------	-----
		.818	1.398	.0249	.9426	35.25	67.4	.879	------	-----
		.819	1.502	.0272	.9386	34.98	67.3	.952	------	-----
(vi)	P	0	1.326	------	------	-----	----	0.845	------	-----
		.805	.997	0.0092	0.9739	36.22	67.2	.334	0.0052	0.566
		[a].801	[a].999	[a].0095	[a].9731	[a]36.13	[a]67.2	[a].345	[a].0060	[a].634
		.801	1.046	.0132	.9707	35.97	67.2	.475	------	-----
		.801	1.100	.0165	.9680	35.43	67.2	.586	------	-----
		.801	1.199	.0213	.9623	35.05	67.4	.748	------	-----
		.801	1.302	.0255	.9570	34.97	67.4	.893	------	-----
		.801	1.397	.0280	.9570	35.75	67.1	1.002	------	-----
(vi)	PAT	0	1.328	------	------	-----	----	1.405	------	-----
		.804	.999	0.0200	0.9669	33.41	68.5	.668	0.0124	0.618
		.803	.999	.0199	.9669	33.64	68.4	.668	.0124	.621
		[a].800	[a].999	[a].0200	[a].9667	[a]33.47	[a]68.5	[a].668	[a].0126	[a].628
		.802	1.048	.0260	.9635	33.43	68.5	.870	------	-----
		.803	1.098	.0307	.9590	33.48	68.4	1.029	------	-----
		.801	1.203	.0397	.9445	32.43	68.6	1.289	------	-----
		.801	1.300	.0448	.9404	33.36	68.2	1.495	------	-----
		.801	1.402	.0506	.9394	33.50	68.0	1.695	------	-----
		.801	1.468	.0555	.9289	32.80	68.2	1.820	------	-----
		.801	1.466	.0549	.9324	33.11	68.2	1.816	------	-----

[a]Data set used for regional flow-rate and loss comparisons.

TABLE II. - Continued.

Configuration	Vane surface region	Velocity ratio, $(V/V_{cr})_{id,3}$	Coolant pressure ratio, p'_c/p'_1	Coolant fraction, Y	Efficiency, η	Equivalent primary flow rate, $w_p\sqrt{\theta_{cr}}/\delta$,	Exit flow angle, α_3, deg	Equivalent coolant flow rate, $w_c\sqrt{\theta_{cr}}/\delta$,	Efficiency loss fraction, $(\eta_0 - \eta)/\eta_0$	Efficiency loss ratio, $(\eta_0 - \eta)/\eta_0 Y$
(vi)	PADT	0	1.329	------	------	-----	----	2.036	------	-----
		[a].815	[a]1.000	[a]0.0358	[a]0.9524	[a]33.66	[a]68.0	[a]1.207	[a]0.0272	[a]0.759
		.818	1.001	.0359	.9527	33.86	67.9	1.216	.0269	.748
		.833	1.050	.0431	.9498	33.89	67.9	1.461	.0298	.692
		.830	1.098	.0489	.9462	33.64	68.0	1.645	.0335	.685
		.832	1.202	.0604	.9331	32.79	68.3	1.982	.0469	.776
		.832	1.299	.0668	.9329	33.80	67.6	2.259	.0471	.705
		.830	1.400	.0794	.9071	31.79	68.4	2.523	.0734	.925
		.828	1.497	.0853	.9039	32.41	68.2	2.764	.0767	.899
(vi)	T	0	1.332	------	------	-----	----	0.077	------	-----
		.811	.945	0.0008	0.9769	35.38	67.8	.029	------	-----
		[a].813	[a]1.001	[a].0017	[a].9770	[a]35.59	[a]67.9	[a].059	[a]0.0020	[a]1.202
		.811	.996	.0016	.9776	35.63	67.8	.055	.0014	.894
		.811	1.052	.0018	.9770	35.80	67.8	.066	------	-----
		.812	1.106	.0020	.9774	35.57	67.8	.071	------	-----
		.812	1.201	.0023	.9772	35.68	67.8	.080	------	-----
		.812	1.309	.0026	.9764	35.41	67.8	.091	------	-----
		.811	1.398	.0028	.9769	35.57	67.8	.100	------	-----
		.811	1.502	.0031	.9769	35.72	67.8	.111	------	-----

(vii)	PADT	0	1.332	------	------	-----	----	2.172	------	-----
		.819	1.001	0.0400	0.9285	32.91	68.1	1.316	0.0516	1.290
		[a].824	[a]1.003	[a].0402	[a].9300	[a]33.16	[a]68.0	[a]1.332	[a].0501	[a]1.245
		.819	1.049	.0477	.9257	32.97	68.0	1.573	.0544	1.141
		.824	1.100	.0541	.9201	33.04	67.9	1.788	.0602	1.112
		.828	1.206	.0668	.9039	32.25	68.1	2.154	.0767	1.148
		.831	1.301	.0770	.8975	31.63	68.5	2.436	.0832	1.081
		.836	1.404	.0870	.8828	31.22	68.4	2.716	.0983	1.129
		.843	1.502	.0936	.8625	31.72	67.9	2.970	.1190	1.271
(viii)	AD	0	1.327	------	------	-----	----	1.036	------	-----
		.786	1.002	0.0227	0.9445	32.91	68.3	.746	0.0352	1.552
		[a].790	[a].999	[a].0225	[a].9466	[a]33.14	[a]68.3	[a].745	[a].0331	[a]1.471
		.831	.999	.0225	.9473	33.88	68.3	.761	.0324	1.439
		.790	1.052	.0256	.9422	33.13	68.3	.848	------	-----
		.790	1.099	.0280	.9410	33.18	68.3	.929	------	-----
		.794	1.200	.0325	.9284	33.06	68.2	1.075	------	-----
		.794	1.302	.0365	.9245	33.14	68.0	1.209	------	-----
		.794	1.501	.0444	.9112	32.75	68.2	1.454	------	-----
(viii)	D	0	1.331	------	------	-----	----	0.591	------	-----
		[a].806	[a].998	[a]0.0146	[a]0.9480	[a]35.50	[a]67.2	[a].518	[a]0.0317	[a]2.169
		.815	1.002	.0143	.9464	35.61	67.1	.509	.0333	2.329
		.805	1.041	.0156	.9454	35.31	67.2	.548	------	-----
		.825	1.104	.0169	.9249	35.00	67.3	.591	------	-----
		.817	1.200	.0184	.9384	35.56	67.0	.652	------	-----
		.817	1.297	.0203	.9273	35.50	66.9	.721	------	-----
		.817	1.400	.0220	.9197	35.68	66.7	.784	------	-----
		.816	1.499	.0238	.9230	35.77	66.8	.852	------	-----

[a]Data set used for regional flow-rate and loss comparisons.

TABLE II. - Concluded.

Configuration	Vane surface region	Velocity ratio, $(V/V_{cr})_{id,3}$	Coolant pressure ratio, p'_c/p'_1	Coolant fraction, Y	Efficiency, η	Equivalent primary flow rate, $w_p\sqrt{\theta_{cr}}/\delta$, (g/sec)/cm	Exit flow angle, α_3, deg	Equivalent coolant flow rate, $w_c\sqrt{\theta_{cr}}/\delta$, (g/sec)/cm	Efficiency loss fraction, $(\eta_0 - \eta)/\eta_0$	Efficiency loss ratio, $(\eta_0 - \eta)/\eta_0 Y$
(viii)	DT	0	1.324	------	------	-----	----	0.652	------	-----
		[a].803	[a]1.001	[a]0.0163	[a]0.9467	[a]34.47	[a]67.7	[a].564	[a]0.0330	[a]2.025
		.816	1.000	.0163	.9461	34.66	67.7	.566	.0336	2.062
		.824	.691	.0058	.9682	35.57	67.8	.205	------	-----
		.825	.794	.0102	.9662	35.34	67.7	.363	------	-----
		.815	.890	.0133	.9561	34.79	67.8	.463	------	-----
		.816	.997	.0162	.9480	34.84	67.7	.566	.0317	1.955
		.816	1.050	.0176	.9449	34.70	67.7	.611	------	-----
		.818	1.098	.0190	.9445	34.34	67.8	.652	------	-----
		.817	1.197	.0211	.9388	34.57	67.6	.729	------	-----
		.818	1.293	.0231	.9303	34.63	67.5	.800	------	-----
		.818	1.364	.0245	.9243	34.72	67.5	.852	------	-----
		.817	1.495	.0275	.9189	34.30	67.7	.943	------	-----
(viii)	P	0	1.327	------	------	-----	----	0.802	------	-----
		[a].827	[a]1.000	[a]0.0099	[a]0.9704	[a]35.45	[a]67.7	[a].350	[a]0.0088	[a]0.887
		.831	1.000	.0100	.9706	35.34	67.7	.352	.0086	.860
		.831	1.051	.0134	.9684	35.73	67.7	.479	------	-----
		.832	1.098	.0159	.9670	35.50	67.7	.564	------	-----
		.834	1.205	.0206	.9610	35.16	67.8	.725	------	-----
		.833	1.298	.0242	.9561	35.00	67.8	.846	------	-----
		.833	1.398	.0277	.9504	34.77	67.8	.963	------	-----
		.832	1.495	.0308	.9443	34.68	67.8	1.070	------	-----

(viii)	PAT	0	1.334	------	------	-----	----	1.316	------	-----
		[a].804	[a]1.000	[a]0.0177	[a]0.9599	[a]35.57	[a]67.3	[a].630	[a]0.0195	[a]1.102
		.814	.949	.0179	.9596	35.23	67.4	.630	.0198	1.107
		.815	1.051	.0236	.9570	35.05	67.4	.829	------	-----
		.801	1.105	.0279	.9489	34.82	67.2	.973	------	-----
		.804	1.192	.0344	.9453	34.61	67.3	1.193	------	-----
		.814	1.302	.0412	.9354	33.98	67.8	1.400	------	-----
		.803	1.403	.0466	.9277	33.91	67.7	1.580	------	-----
		.803	1.494	.0512	.9187	34.05	67.4	1.743	------	-----
(viii)	PADT	0	1.336	------	------	-----	----	1.936	------	-----
		.812	1.000	0.0349	0.9334	33.52	67.8	1.168	0.0466	1.335
		[a].815	[a]1.001	[a].0349	[a].9354	[a]33.61	[a]67.8	[a]1.175	[a].0445	[a]1.276
		.814	1.054	.0424	.9307	33.22	67.9	1.409	.0493	1.164
		.814	1.102	.0480	.9260	32.91	68.0	1.579	..0541	1.128
		.813	1.200	.0579	.9207	32.47	68.2	1.879	.0596	1.029
		.810	1.301	.0652	.9077	32.93	67.6	2.148	.0728	1.117
		.813	1.401	.0721	.8917	33.27	67.3	2.398	.0892	1.237
		.812	1.504	.0807	.8795	32.68	67.4	2.638	.1016	1.259

[a]Data set used for regional flow-rate and loss comparisons.

Vane coordinates		
X	Y_L	Y_U
0	0.508	0.508
.127	-----	.851
.254	-----	1.006
.381	-----	1.123
.508	-----	1.214
.635	-----	1.288
.762	.064	1.346
.889	.119	1.392
1.016	.165	1.427
1.143	.206	1.453
1.270	.241	1.468
1.397	.267	1.473
1.524	.292	1.476
1.778	.330	1.463
2.032	.361	1.433
2.286	.376	1.382
2.540	.384	1.323
2.794	.381	1.257
3.048	.373	1.189
3.302	.353	1.110
3.556	.330	1.031
3.810	.297	.945
4.064	.262	.851
4.318	.221	.747
4.572	.180	.638
4.826	.132	.518
5.080	.081	.391
5.334	.025	.259
5.552	.089	.089

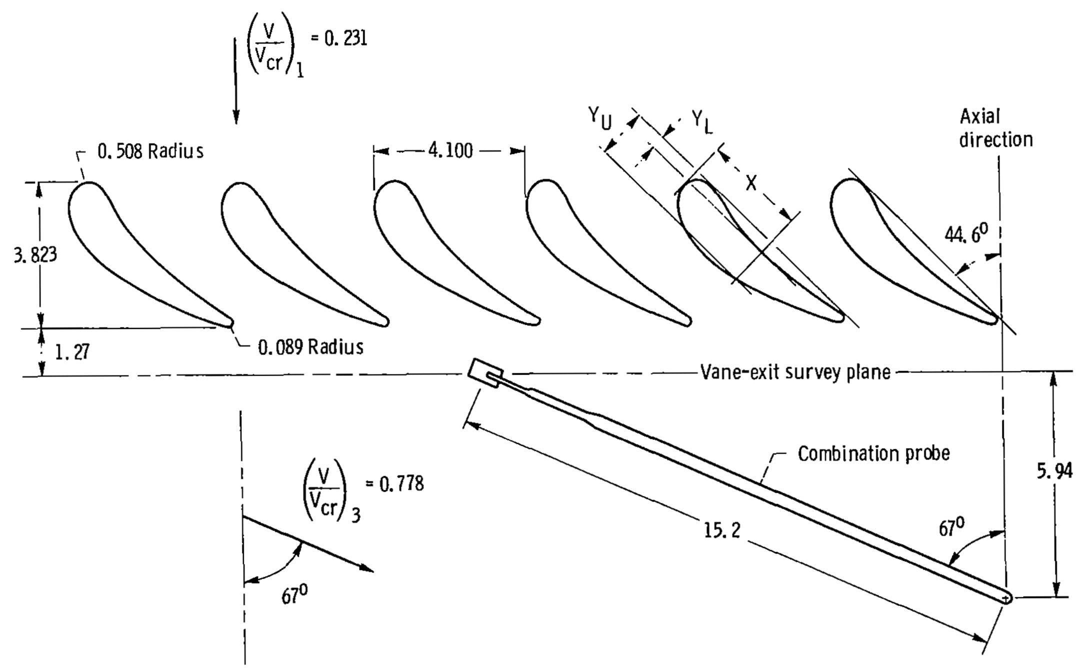

Figure 1. - Cascade geometry and design flow characteristics. (All dimensions are in cm.)

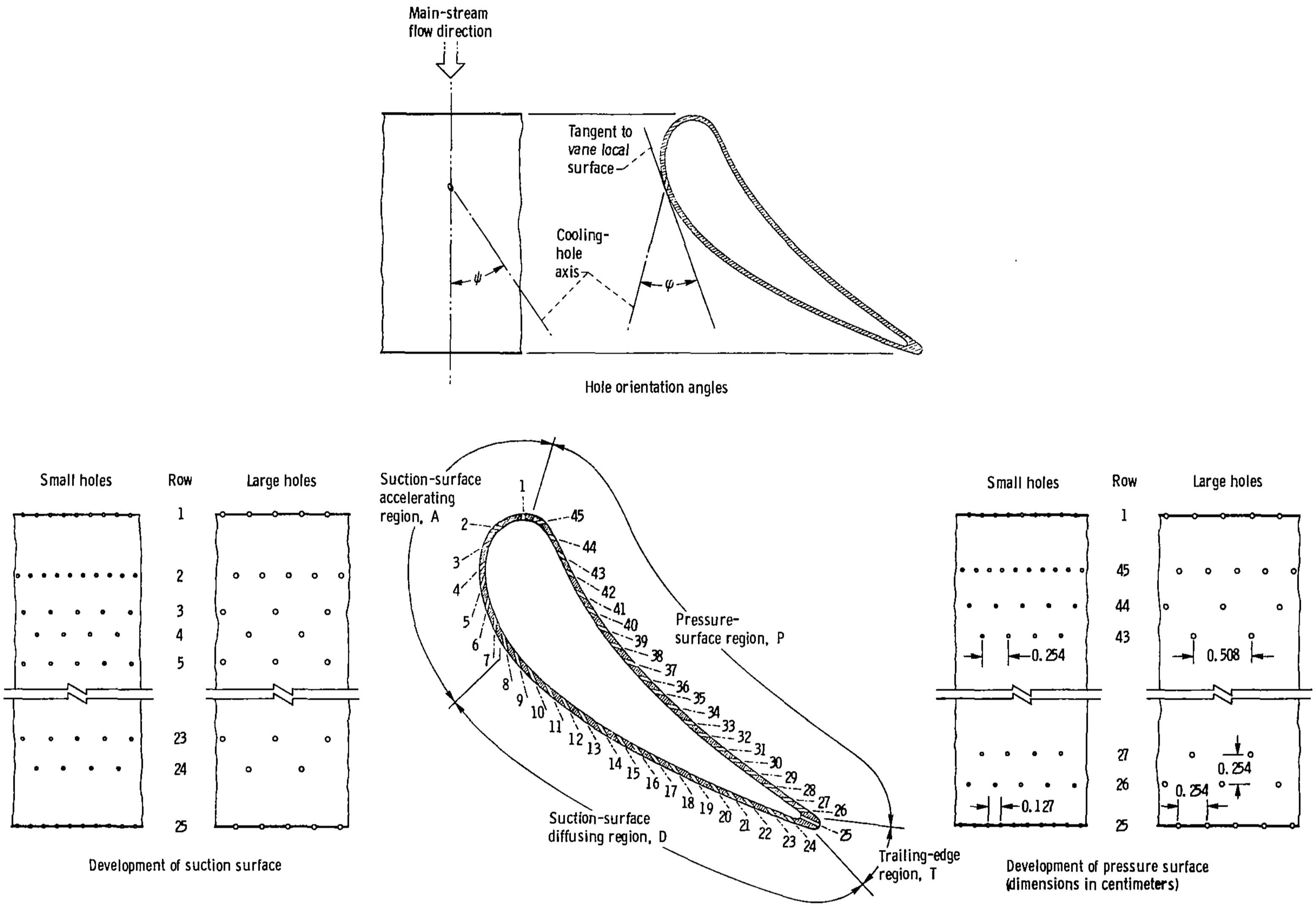

Hole orientation angles

Hole-row location schematic (nominal 35° surface angle configuration shown)

Figure 2. - Schematic of film-cooling hole geometry.

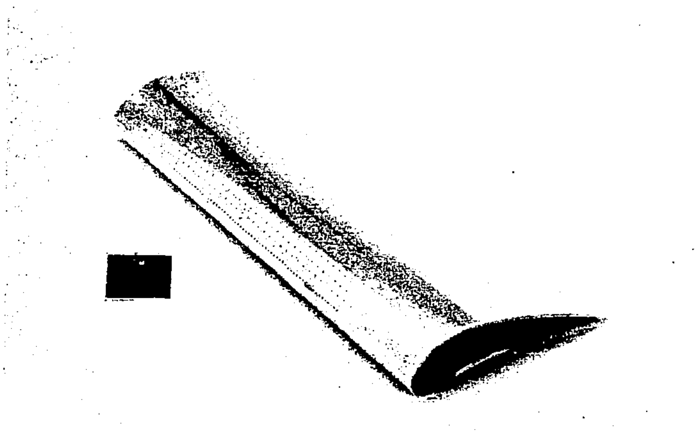

C-75-917

Figure 3. - Configuration (i). Small holes oriented 35° relative to local vane surface and in line with main-stream flow direction.

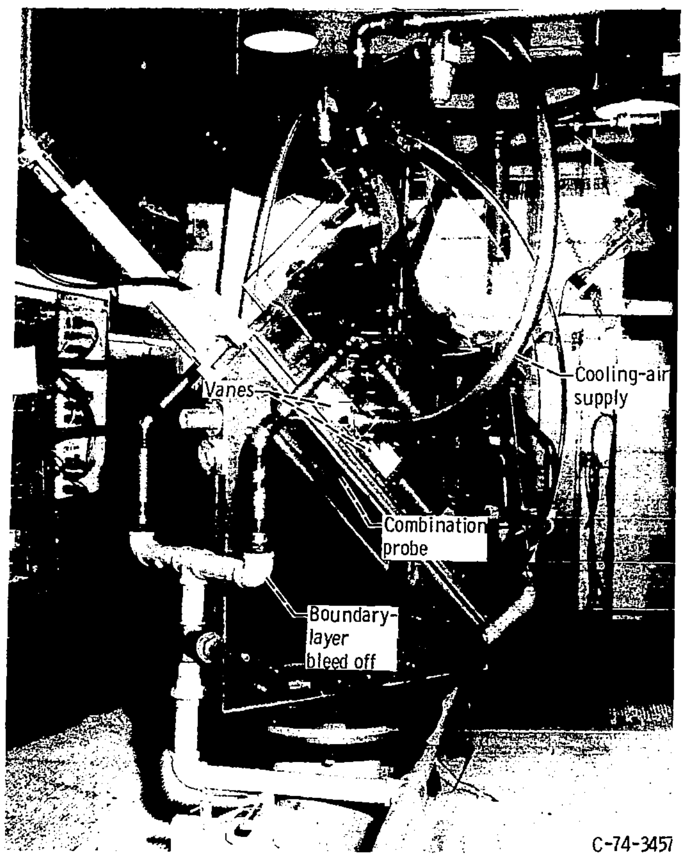

Figure 4. - Two-dimensional cascade tunnel.

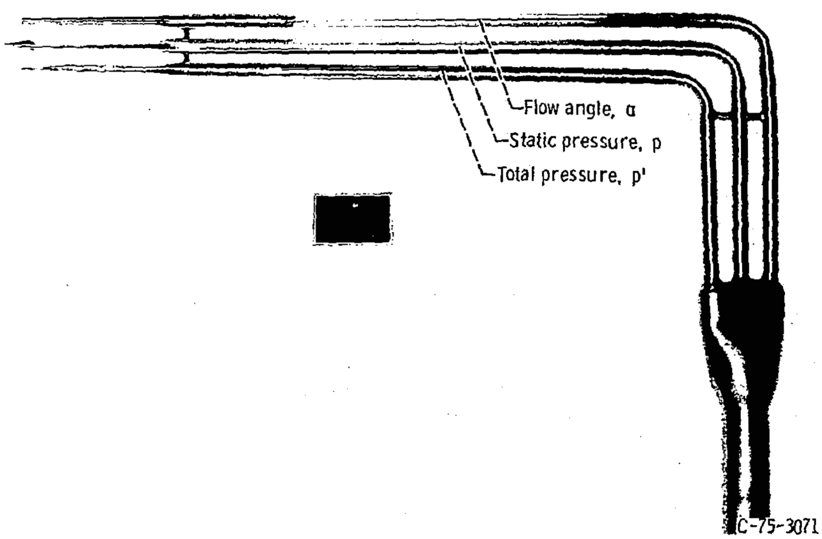

Figure 5. - Combination survey probe.

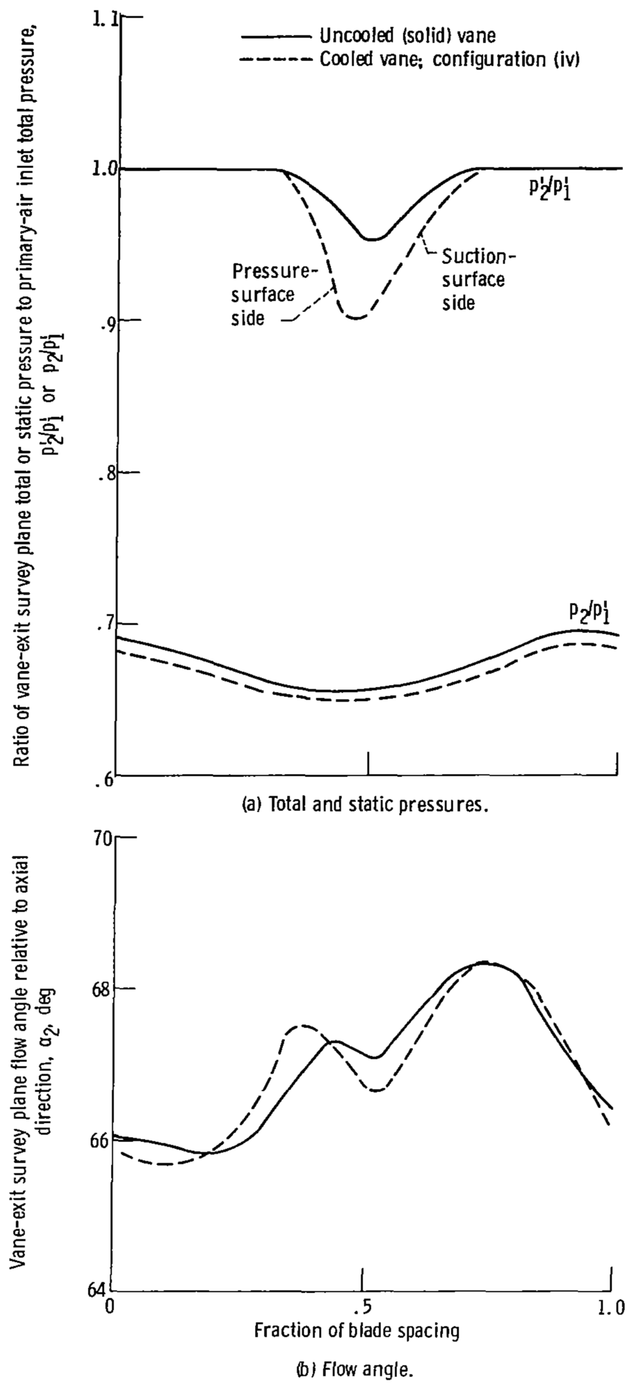

Figure 6. - Vane-to-vane variation of exit survey plane flow conditions of uncooled (solid) vane and cooled vane (configuration (iv); large holes; $\varphi = 35^\circ$; $\psi = 0^\circ$) at design operating conditions.

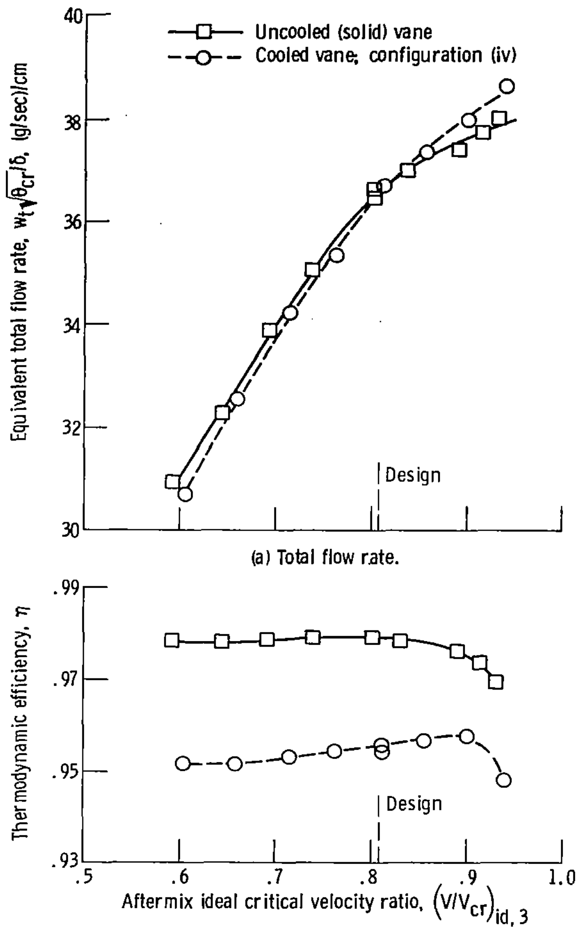

(b) Thermodynamic efficiency.

Figure 7. - Variation of total flow rate and thermodynamic efficiency of uncooled (solid) vane and cooled vane (configuration (iv)) with aftermix ideal critical velocity ratio.

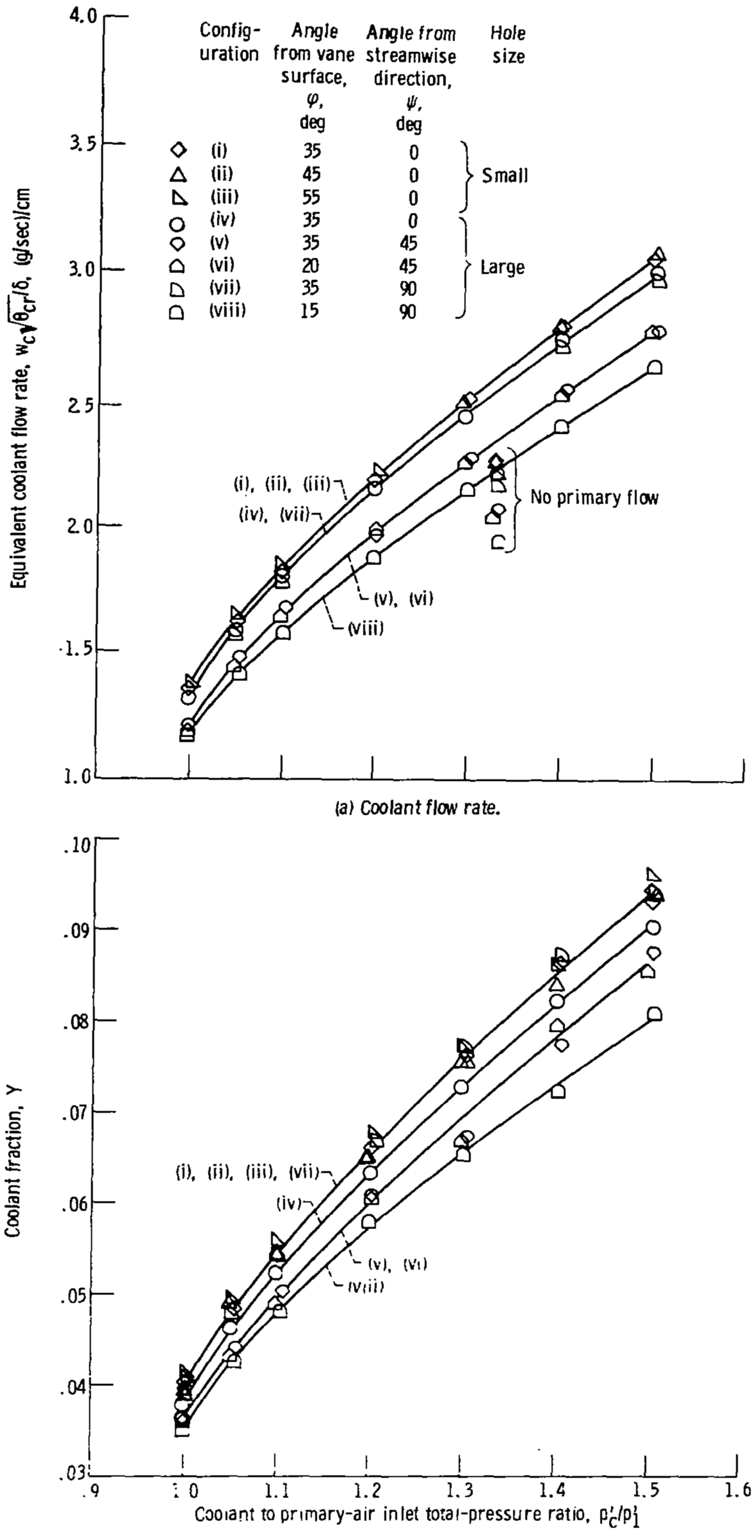

(a) Coolant flow rate.

(b) Coolant flow rate as fraction of primary flow rate.

Figure 8. - Comparison of coolant flow-rate parameters of all configurations.

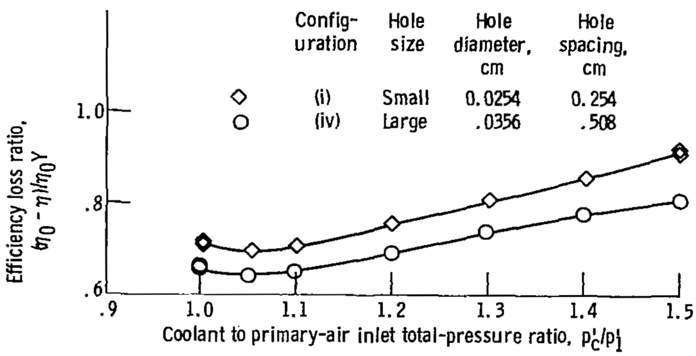

Figure 9. - Effect of hole size on efficiency loss ratio at design aftermix ideal critical velocity ratio $(V/V_{cr})_{id,3}$. Streamwise ($\psi = 0^0$) ejection at 35° from vane surface.

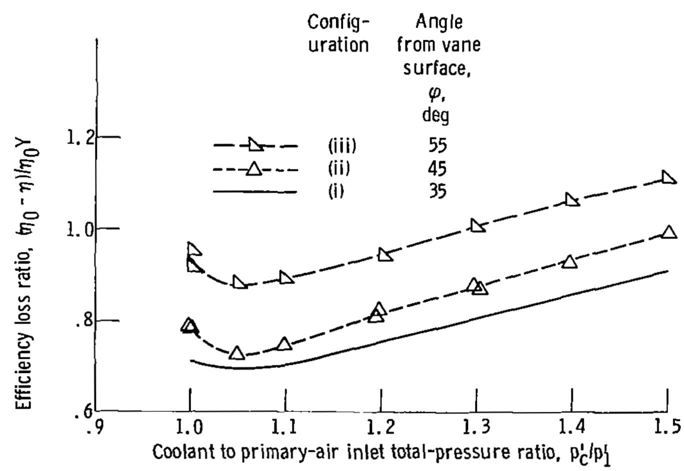

Figure 10. - Effect of ejection angle from vane surface φ on efficiency loss ratio at design aftermix ideal critical velocity ratio $(V/V_{cr})_{id,3}$. Streamwise ($\psi = 0^0$) ejection from small holes.

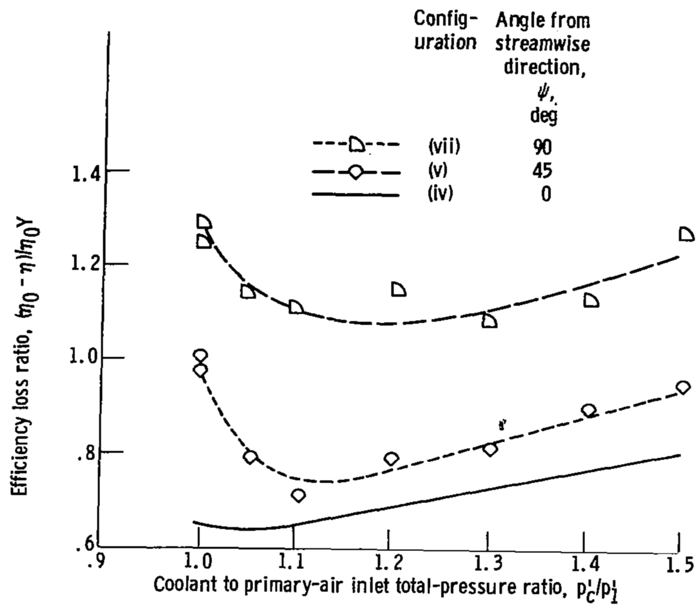

Figure 11. - Effect of ejection angle from streamwise direction ψ on efficiency loss ratio at design aftermix ideal critical velocity ratio $(V/V_{cr})_{id,3}$. Ejection from large holes at 35° from vane surface.

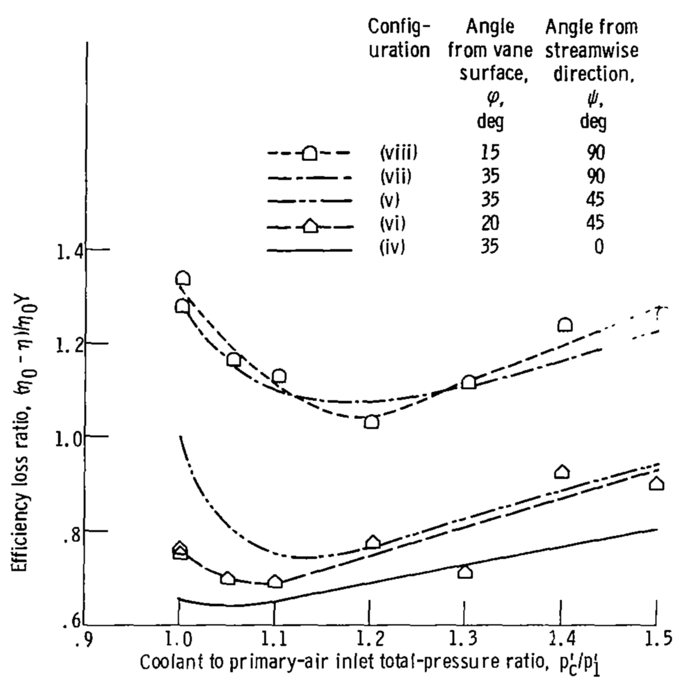

Figure 12. - Effect of smaller ejection angles from the vane surface on efficiency loss ratio for compound-angle ejection from large holes at design aftermix ideal critical velocity ratio $(V/V_{cr})_{id,3}$.

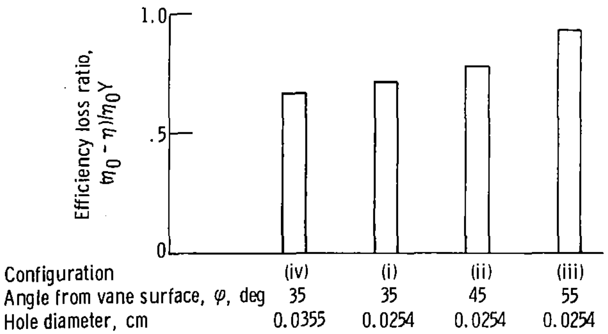

(a) Streamwise ejection ($\psi = 0^0$).

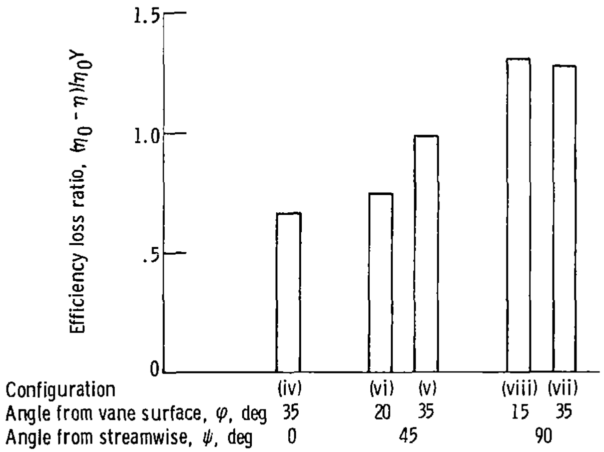

(b) Compound-angle ejection.

Figure 13. - Summary of ejection geometry effects on vane efficiency at a coolant to primary-air inlet total-pressure ratio p_c'/p_1' of 1.0 and design aftermix ideal critical velocity ratio $(V/V_{cr})_{id,3}$.

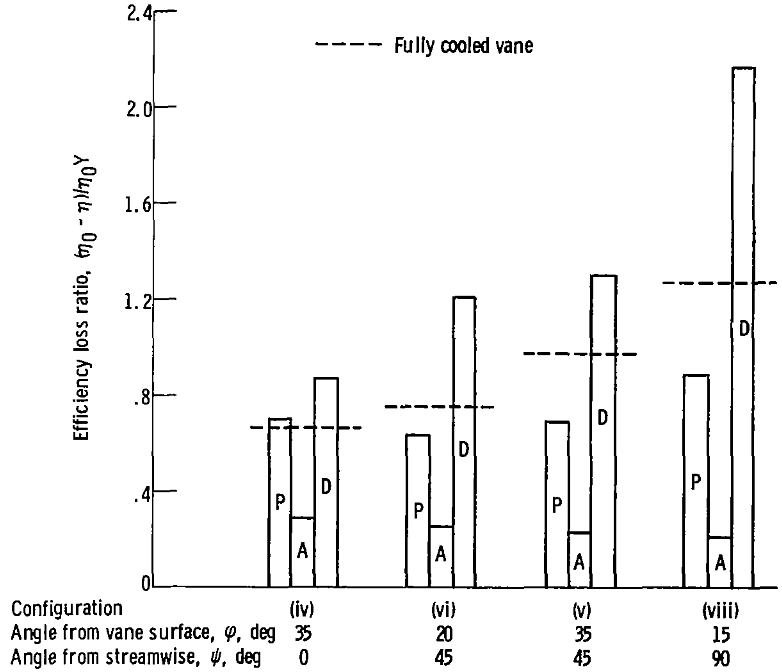

Figure 14. - Efficiency loss ratio for ejection from individual surface regions at a coolant to primary air inlet total pressure ratio p_c'/p_1' of 1.0 and design aftermix ideal critical velocity ratio $(V/V_{cr})_{id,3}$.

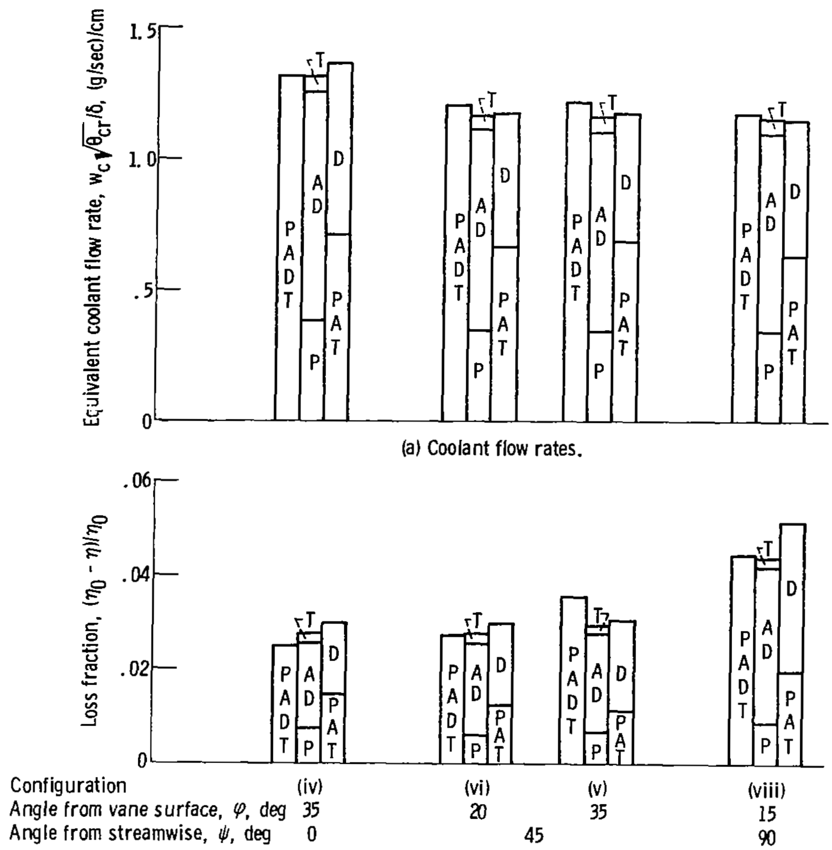

(b) Cooling losses.

Figure 15. - Additive characteristics of regional flow rates and losses.

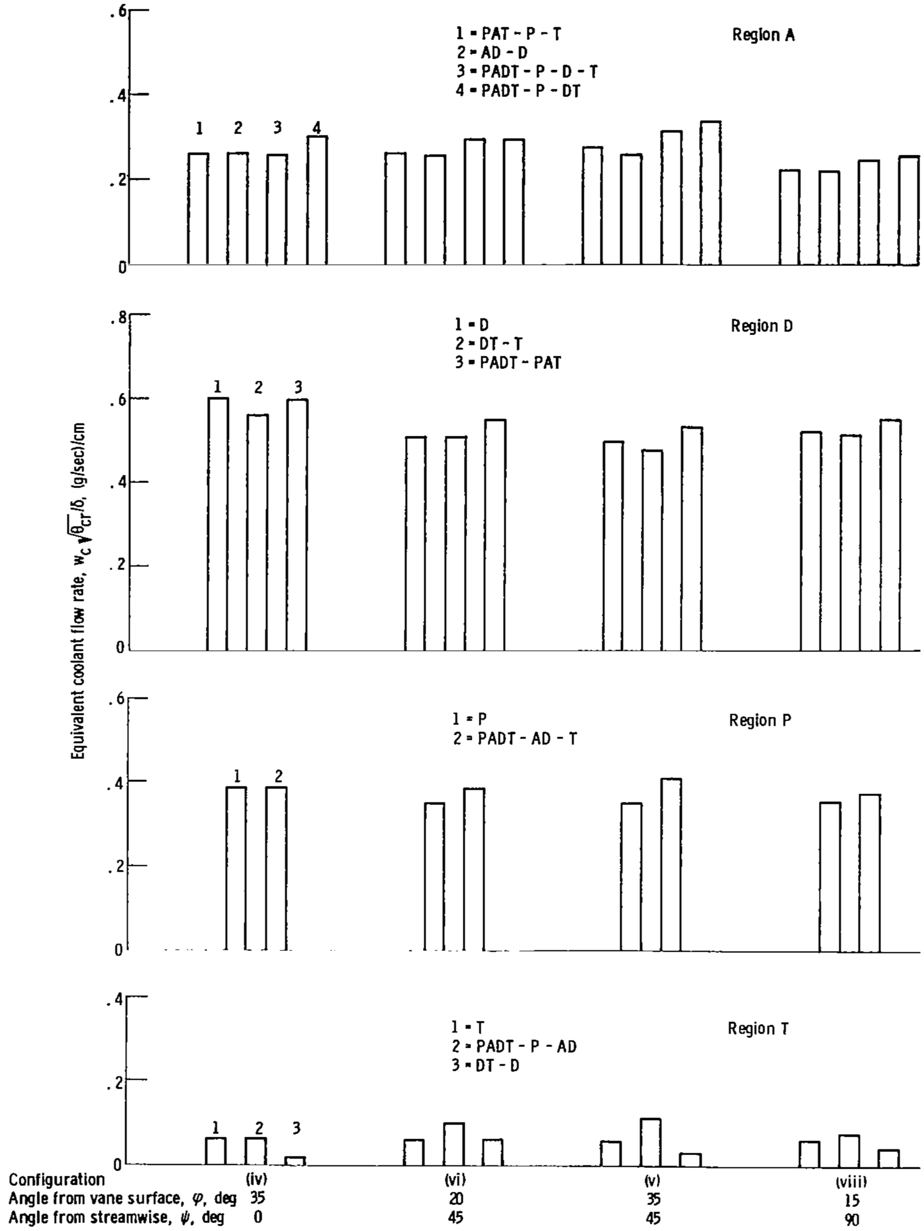

(a) Coolant flow rate.

Figure 16. - Regional flow rate and loss comparisons.

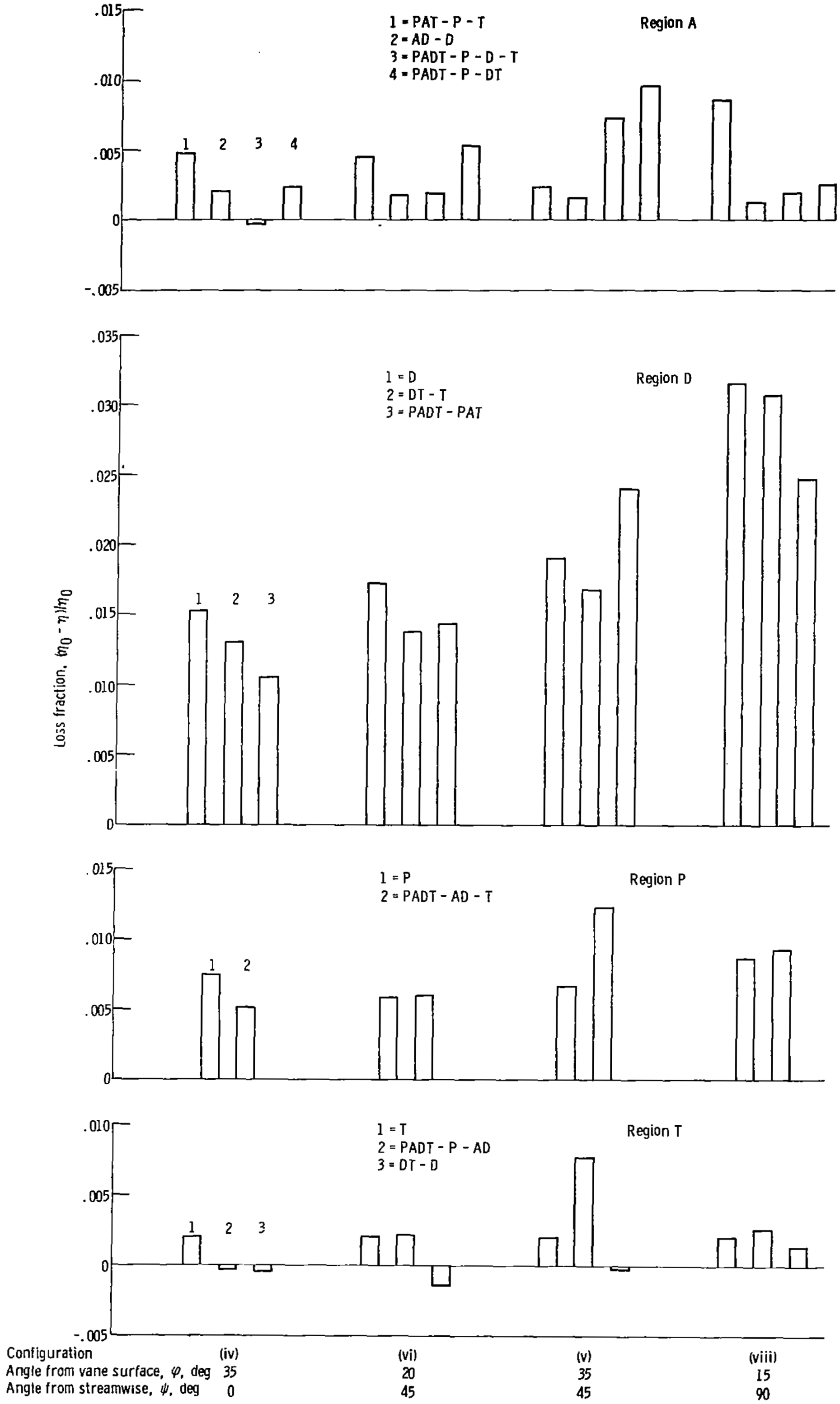

(b) Cooling losses.

Figure 16. - Concluded.

1. Report No. NASA TP-1136	2. Government Accession No.	3. Recipient's Catalog No.
4. Title and Subtitle EFFECT OF COOLING-HOLE GEOMETRY ON AERODYNAMIC PERFORMANCE OF A FILM-COOLED TURBINE VANE TESTED WITH COLD AIR IN A TWO-DIMENSIONAL CASCADE		5. Report Date March 1978
		6. Performing Organization Code
7. Author(s) John F. Kline, Roy G. Stabe, and Thomas P. Moffitt		8. Performing Organization Report No. E-9174
		10. Work Unit No. 505-04
9. Performing Organization Name and Address National Aeronautics and Space Administration Lewis Research Center Cleveland, Ohio 44135		11. Contract or Grant No.
		13. Type of Report and Period Covered Technical Paper
12. Sponsoring Agency Name and Address National Aeronautics and Space Administration Washington, D.C. 20546		14. Sponsoring Agency Code
15. Supplementary Notes		

16. Abstract

The effect of cooling-hole size and orientation on turbine-vane aerodynamic losses was evaluated. The contribution of individual vane regions to the overall effect was also investigated. Test configurations were based upon a representative configuration having 45 spanwise rows of holes spaced about the entire vane profile. Nominal hole diameters of 0.0254 and 0.0356 cm and nominal hole orientations of 35°, 45°, and 55° from the local vane surface and 0°, 45°, and 90° from the main-stream flow direction were investigated. Flow conditions and aerodynamic losses were determined by vane-exit surveys of total pressure, static pressure, and flow angle.

17. Key Words (Suggested by Author(s))	18. Distribution Statement
Turbine Cooling Aerodynamics	Unclassified - unlimited STAR Category 02

19. Security Classif. (of this report)	20. Security Classif. (of this page)	21. No. of Pages	22. Price*
Unclassified	Unclassified	47	A03

* For sale by the National Technical Information Service, Springfield, Virginia 22161

NASA-Langley, 1978